



ELSEVIER

Contents lists available at ScienceDirect

## Data in brief

journal homepage: [www.elsevier.com/locate/dib](http://www.elsevier.com/locate/dib)

## Data Article

## Experimental data on novel Fe(III)-complexes containing phenanthroline derivatives for their anticancer properties



Cristina P. Matos <sup>a,1</sup>, Zelal Adiguzel <sup>b,1</sup>, Yasemin Yildizhan <sup>b,1</sup>,  
 Buse Cevatemre <sup>c</sup>, Tugba Bagci-Onder <sup>c,d</sup>, Ozge Cevik <sup>e</sup>,  
 Patrique Nunes <sup>a</sup>, Liliana P. Ferreira <sup>f,g</sup>, Maria Deus Carvalho <sup>h</sup>,  
 Débora L. Campos <sup>i</sup>, Fernando R. Pavan <sup>i</sup>, João Costa Pessoa <sup>a</sup>,  
 Maria Helena Garcia <sup>j</sup>, Ana Isabel Tomaz <sup>j</sup>, Isabel Correia <sup>a,\*</sup>,  
 Ceyda Acilan <sup>c,d,\*\*</sup>

<sup>a</sup> Centro de Química Estrutural, Instituto Superior Técnico, Departamento de Engenharia Química, Universidade de Lisboa, Av. Rovisco Pais 1, 1049-001, Lisboa, Portugal

<sup>b</sup> TUBITAK, Marmara Research Center, Genetic Engineering and Biotechnology Institute, Gebze, Kocaeli, Turkey

<sup>c</sup> Koc University Research Center for Translational Medicine (KUTTAM), Sariyer, Istanbul, Turkey

<sup>d</sup> Koc University, Medical School, Sariyer, Istanbul, Turkey

<sup>e</sup> Adnan Menderes University, School of Medicine, Aydin, Turkey

<sup>f</sup> BioISI, Faculdade de Ciências, Universidade de Lisboa, Campo Grande, 1749-016 Lisboa, Portugal

<sup>g</sup> Department of Physics, University of Coimbra, 3004-516 Coimbra, Portugal

<sup>h</sup> Centro de Química e Bioquímica, Faculdade de Ciências, Universidade de Lisboa, Campo Grande, 1749-016 Lisboa, Portugal

<sup>i</sup> Faculdade de Ciências Farmacêuticas, UNESP, C.P.582, Araraquara, SP 14801-902, Brazil

<sup>j</sup> Centro de Química Estrutural, Faculdade de Ciências, Universidade de Lisboa, Campo Grande, 1749-016 Lisbon, Portugal

DOI of original article: <https://doi.org/10.1016/j.ejmech.2019.04.070>.

\* Corresponding author.

\*\* Corresponding author. Koc University, Medical School, Sariyer, Istanbul, Turkey.

E-mail addresses: [cristina.matos@tecnico.ulisboa.pt](mailto:cristina.matos@tecnico.ulisboa.pt) (C.P. Matos), [zelal.adiguzel@tubitak.gov.tr](mailto:zelal.adiguzel@tubitak.gov.tr) (Z. Adiguzel), [yasemin.yildizhan@tubitak.gov.tr](mailto:yasemin.yildizhan@tubitak.gov.tr) (Y. Yildizhan), [bcevatemre@ku.edu.tr](mailto:bcevatemre@ku.edu.tr) (B. Cevatemre), [tuonder@ku.edu.tr](mailto:tuonder@ku.edu.tr) (T. Bagci-Onder), [ozge.cevik@adu.edu.tr](mailto:ozge.cevik@adu.edu.tr) (O. Cevik), [patrique.nunes@tecnico.ulisboa.pt](mailto:patrique.nunes@tecnico.ulisboa.pt) (P. Nunes), [lmferreira@fc.ul.pt](mailto:lmferreira@fc.ul.pt) (L.P. Ferreira), [mdcarvalho@fc.ul.pt](mailto:mdcarvalho@fc.ul.pt) (M.D. Carvalho), [leite.debora26@gmail.com](mailto:leite.debora26@gmail.com) (D.L. Campos), [fernandopavan@fcfar.unesp.br](mailto:fernandopavan@fcfar.unesp.br) (F.R. Pavan), [joao.pessoa@tecnico.ulisboa.pt](mailto:joao.pessoa@tecnico.ulisboa.pt) (J.C. Pessoa), [mhgarcia@fc.ul.pt](mailto:mhgarcia@fc.ul.pt) (M.H. Garcia), [isabel.tomaz@fc.ul.pt](mailto:isabel.tomaz@fc.ul.pt) (A.I. Tomaz), [icorreia@tecnico.ulisboa.pt](mailto:icorreia@tecnico.ulisboa.pt) (I. Correia), [cayhan@ku.edu.tr](mailto:cayhan@ku.edu.tr) (C. Acilan).

<sup>1</sup> These authors contributed equally to this work.

<https://doi.org/10.1016/j.dib.2019.104548>

2352-3409/© 2019 The Author(s). Published by Elsevier Inc. This is an open access article under the CC BY-NC-ND license (<http://creativecommons.org/licenses/by-nc-nd/4.0/>).

## ARTICLE INFO

## Article history:

Received 9 May 2019

Received in revised form 29 August 2019

Accepted 13 September 2019

Available online 27 September 2019

## Keywords:

Fe(III) complexes

Phenanthroline

Anticancer

Cytotoxicity

Genotoxicity

## ABSTRACT

This dataset is related to the research article entitled “May iron(III) complexes containing phenanthroline derivatives as ligands be prospective anticancer agents?” [1]. It includes the characterization by UV–Vis absorption spectroscopy and magnetic techniques of a group of mixed ligand Fe(III) complexes bearing a tripodal amino-phenolate ligand  $L^{2-}$ ,  $H_2L = N,N$ -bis(2-hydroxy-3,5-dimethylbenzyl)- $N$ -(2-pyridylmethyl)amine, and different aromatic bases (NN = 2,2′-bipyridine [Fe(L)(bipy)]PF<sub>6</sub> (**1**), 1,10-phenanthroline [Fe(L)(phen)]PF<sub>6</sub> (**2**), or a phenanthroline derivative co-ligand: [Fe(L)(amphen)]NO<sub>3</sub> (**3**), [Fe(L)(amphen)]PF<sub>6</sub> (**3a**), [Fe(L)(Clphen)]PF<sub>6</sub> (**4**), [Fe(L)(epoxyphen)]PF<sub>6</sub> (**5**) (where amphen = 1,10-phenanthroline-5-amine, epoxyphen = 5,6-epoxy-5,6-dihydro-1,10-phenanthroline, Clphen = 5-chloro-1,10-phenanthroline), as well as [Fe(L)(EtOH)]NO<sub>3</sub> (**6**), [Fe(phen)Cl<sub>3</sub>] (**7**) and [Fe(amphen)Cl<sub>3</sub>] (**8**). Data on their hydrolytic stability in physiological buffers is shown, as well as on their interaction with *calf thymus* DNA by spectroscopic tools. Additionally, the anticancer efficacy and the cellular death mechanisms activated in response to these drugs in HeLa, H1299 and MDA-MB-231 cells are provided.

© 2019 The Author(s). Published by Elsevier Inc. This is an open access article under the CC BY-NC-ND license (<http://creativecommons.org/licenses/by-nc-nd/4.0/>).

## Specifications Table

Subject area	Chemistry, Biology
More specific subject area	Iron(III) complexes, DNA binding, Structural and Molecular biology, Cancer biology, Drug development
Type of data	Tables, microscopic images, figures
How data was acquired	Circular dichroism (Jasco 720), UV–Vis absorption (Perkin Elmer Lambda 35), Fluorescence (SPEX® Fluorolog spectrofluorometer from Horiba Jobin Yvon), luminometer, fluorescence microscope, flow cytometry.
Data format	Analyzed
Experimental factors	Fe(III) complexes solutions were titrated with <i>Calf thymus</i> DNA. HeLa, H1299 and MDA-MB-231 cells were treated with Fe(III) complexes and incubated at 37 °C and 5% CO <sub>2</sub> .
Experimental features	Fe(III)-complexes spectroscopic and magnetic features: hydrolytic stability and DNA binding evaluated by Circular Dichroism, UV–Vis absorption and fluorescence spectroscopy. The mode of cell death was determined through TUNEL and COMET assays, Annexin V/7AAD and H2AX/8-oxo-Guanine stainings, Caspase 3/7 activity and DCFDA analysis.
Data source location	Koc University School of Medicine, Istanbul/Turkey and Centro de Química Estrutural/IST/Lisbon/Portugal
Data accessibility	Data are supplied with this article.
Related research article	C.P. Matos, Z. Adiguzel, Y. Yildizhan, B. Cevatemre, T. Bagci Onder, O. Cevik, P. Nunes, L. P. Ferreira, M. D. Carvalho, D. L. Campos, F. R. Pavan, J. Costa Pessoa, M. Helena Garcia, A. I. Tomaz, I. Correia*, C. Acilan*, May iron(III) complexes containing phenanthroline derivatives as ligands be prospective anticancer agents?, Eur. J. Med. Chem. 176 (2019) 492–512 [1].

## Value of the Data

- The dataset herein may give researchers in anticancer drug development field a reference for comparison with similar compounds or with complexes carrying similar ligands.
- The data provides additional insight through confirmation of results in two cell lines in addition to the cell line used in the main study (cervix). This may be particularly useful for scientists, who are interested in lung and breast cancer research.
- The data is relevant for chemists interested in the hydrolytic stability of Fe(III) complexes and in the cytotoxicity of ternary Fe(III) complexes containing phenanthroline co-ligands.
- The data may be relevant for researchers using Fe(III) complexes for further mechanistic studies that focus on growth inhibition as a result of apoptosis.

## 1. Data

The introduction of a NN aromatic heterocyclic co-ligand, with NN = 2,2'-bipyridine (bipy), 1,10-phenanthroline (phen) or a 1,10-phenanthroline derivative, in the Fe-coordination sphere, may reinforce their biological activity. Anticancer drugs can exert therapeutic effects through several mechanisms, and the mode of action of Fe(III)-complexes is still matter of debate, with multiple molecular targets possibly being involved. Here we report experimental data on characterization of Fe(III) complexes and their mode of action on human cancer cell lines.

The Fe-aminophenolate complexes [1] were characterized by UV–Vis spectroscopy in different solvents (Figs. 1–4), which allowed the assignment of their spectral bands. Their characterization by magnetic techniques – magnetization *versus* temperature measurements (Fig. 5) and Mössbauer spectroscopy (Fig. 6) - identified them as high spin Fe(III) species.

When developing metallodrugs, species with adequate stability and defined hydrolytic products are required. As metal complexes may suffer aquation, hydrolysis and ligand exchange, information on their hydrolytic stability is of utmost importance. Monitorization of UV–Vis spectral changes of the complexes in buffers (pH = 7.4) was done (Fig. 7) as well as by ESI-MS spectrometry (Fig. 8 and Table 1).

DNA may be a target for the metallodrugs, since phenanthroline molecules are known to intercalate between DNA base pairs. Thus, to elucidate the capability of all compounds to bind DNA, spectroscopic studies were done by circular dichroism (Figs. 9 and 10), UV–Vis absorption (Figs. 11 and 12) and fluorescence (Fig. 13).

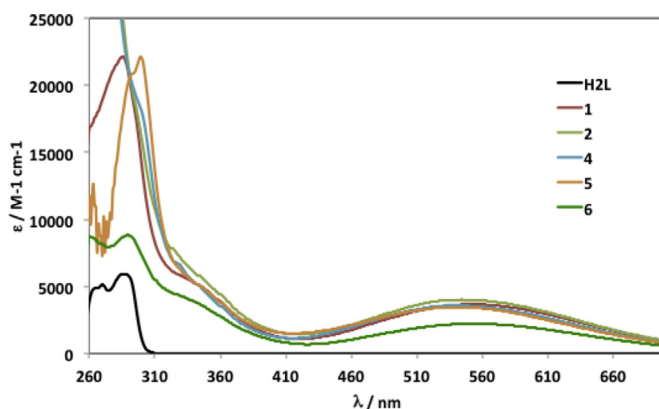


Fig. 1. UV–Vis spectra of H<sub>2</sub>L and complexes 1–6 in DMSO.

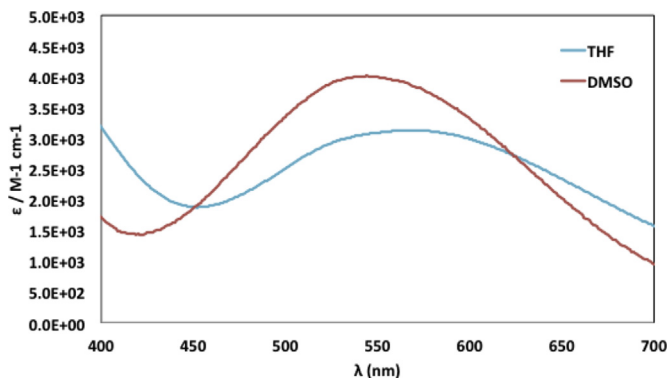


Fig. 2. Vis spectra of complex 3 in THF and DMSO, evidencing the solvatochromic shift observed in the LMCT band.

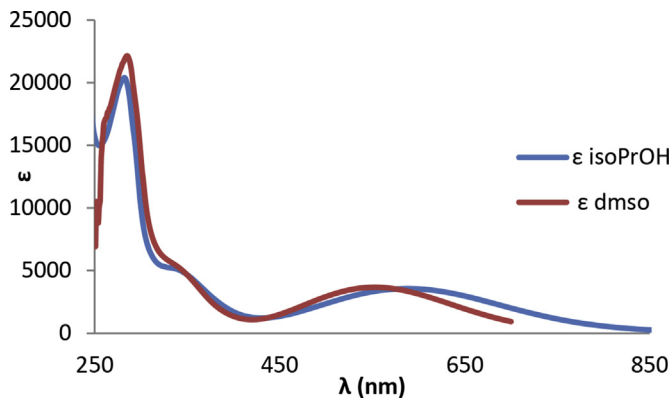


Fig. 3. UV-Vis spectra of complex 1 in isopropanol and DMSO, evidencing the solvathochromic shift.  $\epsilon$  in  $M^{-1} cm^{-1}$ .

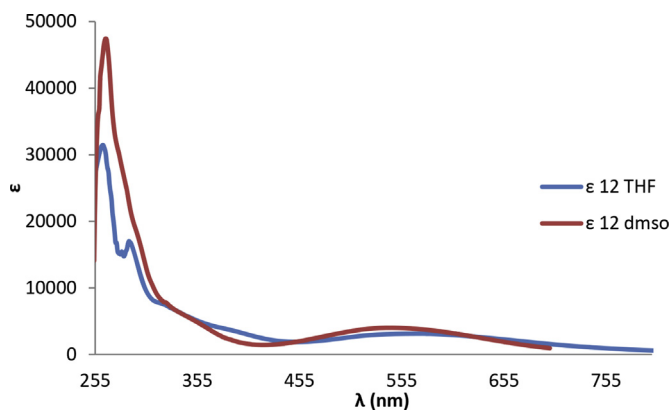


Fig. 4. UV-Vis spectra of complex 2 in isopropanol and THF, evidencing the solvathochromic shift.  $\epsilon$  in  $M^{-1} cm^{-1}$ .

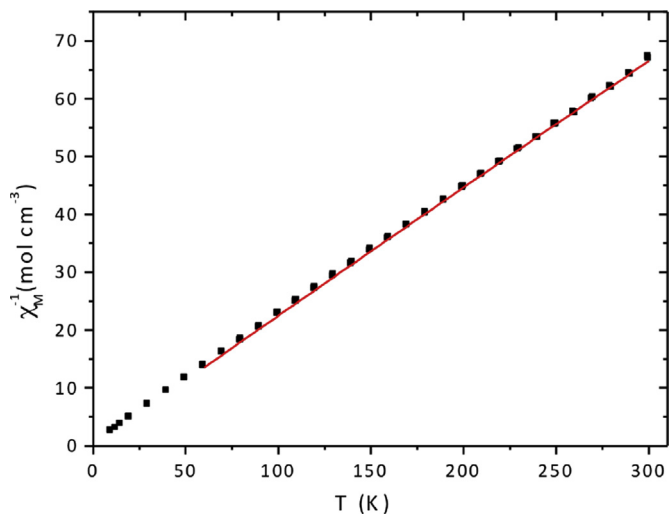
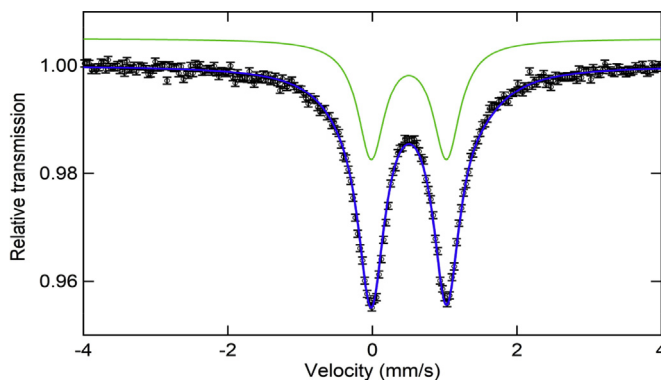


Fig. 5. Temperature dependence of the inverse molar magnetic susceptibility for  $[Fe(L)(phen)]PF_6$  (2). The straight line was obtained from the Curie law fitting to the experimental values.



**Fig. 6.**  $^{57}\text{Fe}$  Mössbauer spectrum of  $[\text{Fe}(\text{L})(\text{EtOH})]\text{NO}_3$  (**6**), collected at 78 K. The spectrum was recorded in transmission mode using a conventional constant-acceleration spectrometer and a 50 mCi  $^{57}\text{Co}$  source in a Rh matrix. The velocity scale was calibrated using an  $\alpha$ -Fe foil. The spectrum was fitted to Lorentzian lines using the WinNormos software program, and the isomer shift reported is relative to metallic  $\alpha$ -Fe at room temperature.

During the execution of apoptosis, cells display marked morphological features such as shrinkage, blebbing or formation of blisters [2]. Many examples of cellular blebs, which appeared as balloon-like protrusions on the membrane, were detected in H1299 and MDA-MB-231 cells (Fig. 14). Cellular shrinkage and decrease in cell numbers were also evident in a concentration (6.3–50  $\mu\text{M}$ ) and time (24, 72 h) dependent manner for all cell lines (Figs. 15–17).

The data on apoptosis was confirmed through the assessment of degradation of DNA (TUNEL assay) (Fig. 18), Annexin V staining (Fig. 19) and caspase 3/7 activity (Fig. 20) in these cells.

The increase in oxidative stress was evaluated by the measurement of intracellular DCFDA (Figs. 21A and 22A) and the examination of 8-oxo-G staining (Figs. 21B and 22B) in H1299 and MDA-MB-231 cells. All complexes (**2**, **3** and **4**) triggered phosphorylation of H2AX confirming that DSBs were induced in cells (Fig. 23, H1299 cells) (Fig. 24, MDA-MB-231 cells). The genotoxicity and effectiveness exerted by these complexes were also evaluated, H1299 (Fig. 25) and MDA-MB-231 (Fig. 26) cells exhibited comet formation with increasing DNA tail percentage in a dose dependent manner (0, 12.5 and 25  $\mu\text{M}$ ).

## 2. Experimental design, materials and methods

### 2.1. Characterization of the complexes

Electronic absorption spectra (UV–Vis) were recorded with a Perkin Elmer Lambda 35 spectrometer in DMSO, isopropanol or THF. Magnetisation measurements as a function of temperature were performed using a SQUID magnetometer (Quantum Design MPMS). The curves were obtained at 0.1 T for temperatures ranging from 10 to 300 K. The molar susceptibilities values were corrected for diamagnetism of the constituent atoms.

### 2.2. Hydrolytic stability

Electronic absorption spectra (UV–Vis) were recorded with time for complexes dissolved in 3% DMSO/97% Hepes (10 mM, pH 7.4). A LCQ Fleet™ Ion Trap Mass Spectrometer from Thermo Scientific was used to measure ESI-MS spectra of methanolic solutions of the complexes in the positive mode for characterization, and of aqueous solutions (3% DMSO- $\text{NaHCO}_3$  aqueous buffer pH 7.4) for stability experiments.

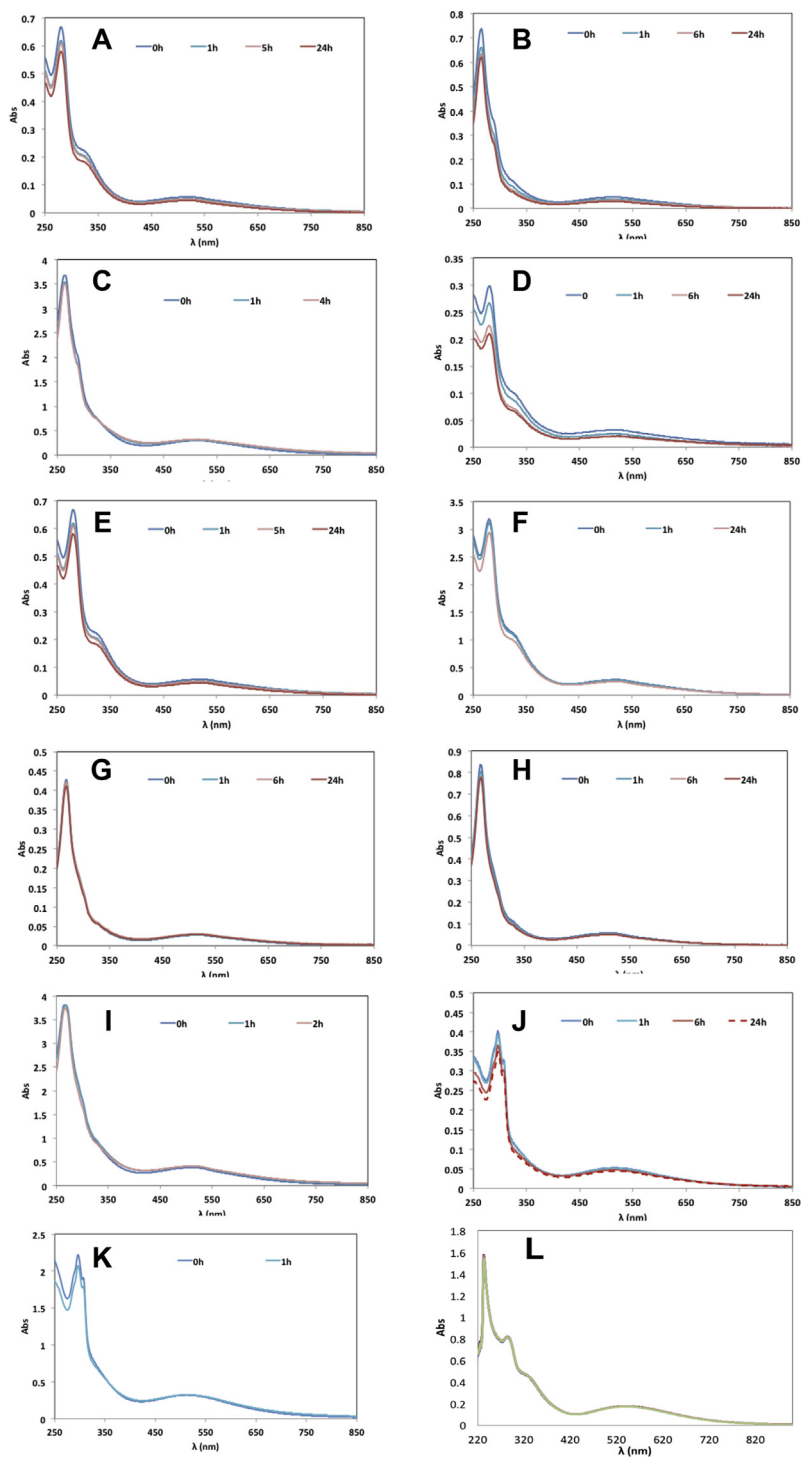


**Fig. 7.** Evaluation of the complexes' stability by UV-Vis spectroscopy at different concentrations and time intervals (indicated in the figures) in 3% DMSO -Hepes (10mM, pH 7.4): (A) **2**, 10 mM; (B) **2**, 20 mM; (C) **2**, 100 mM; (D) **3**, 10 mM; (E) **3**, 20 mM; (F) **3**, 100 mM; (G) **4**, 10mM; (H) **4**, 20mM; (I) **4**, 100mM; (J) **5**, 20 mM; (K) **5**, 100 mM; (L) **6**, 100 mM in 2% DMSO-water.

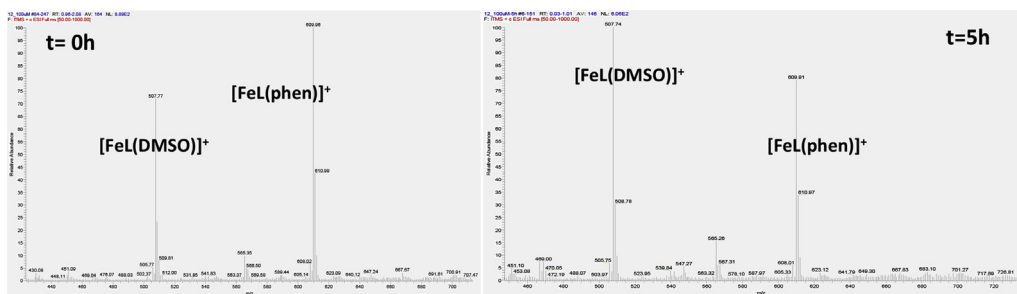


**Fig. 8.** ESI-MS spectra of complex **2**, 100 mM in 3%DMSO-NaHCO<sub>3</sub> buffer (25mM, pH = 7.4) at time 0 and 5 h, showing the increase in the peak assigned to a solvation species [Fe(L)(DMSO)]<sup>+</sup>.

**Table 1**

ESI-MS evaluation of the complexes' stability in 3% DMSO-NaHCO<sub>3</sub> buffer (25mM, pH = 7.4), during 24 h.

Mass observed ( <i>m/z</i> )	Assignment	T = 0 (%)	T = 2h (%)	T = 5h (%)	T = 24h (%)
<b>2</b>					
610.99	[Fe(L)(phen)] <sup>+</sup>	20	10	9	5
507.77	[Fe(L)(DMSO)] <sup>+</sup>	15	10	10	5
377.06	LH <sup>+</sup>	25	22	5	3
181.03	phen <sup>+</sup>	90	100	100	100
<b>3</b>					
624.98	[Fe(L)(amphen)] <sup>+</sup>	10	8	5	4
507.75	[Fe(L)(DMSO)] <sup>+</sup>	7	10	7	5
377.05	LH <sup>+</sup>	15	20	10	2
196.08	amphen <sup>+</sup>	55	80	80	70
<b>4</b>					
643.89	[Fe(L)(Clphen)] <sup>+</sup>	5	5	4	2
507.75	[Fe(L)(DMSO)] <sup>+</sup>	10	10	7	5
377.05	LH <sup>+</sup>	35	30	22	2
215.08	Clphen <sup>+</sup>	60	82	60	30
<b>5</b>					
625.94	[Fe(L)(epoxyphen)] <sup>+</sup>	5	3	1	1
507.75	[Fe(L)(DMSO)] <sup>+</sup>	10	10	7	5
377.05	LH <sup>+</sup>	42	17	20	2
197.08	epoxyphen <sup>+</sup>	56	65	30	30

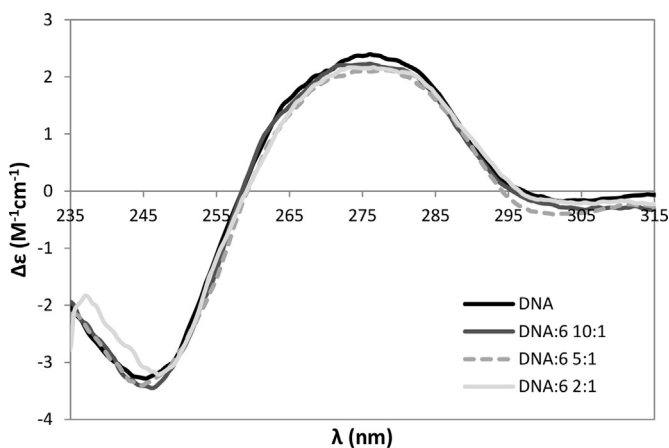


**Fig. 9.** Circular dichroism spectra of ctDNA (80 μM) in the absence and presence of increasing amounts of **6**, [Fe(L)(EtOH)]NO<sub>3</sub>, in DMSO-Hepes 10 mM (pH 7.4). The formation of small "aggregates" in solution was observed for DNA/complex ratio of 2:1.

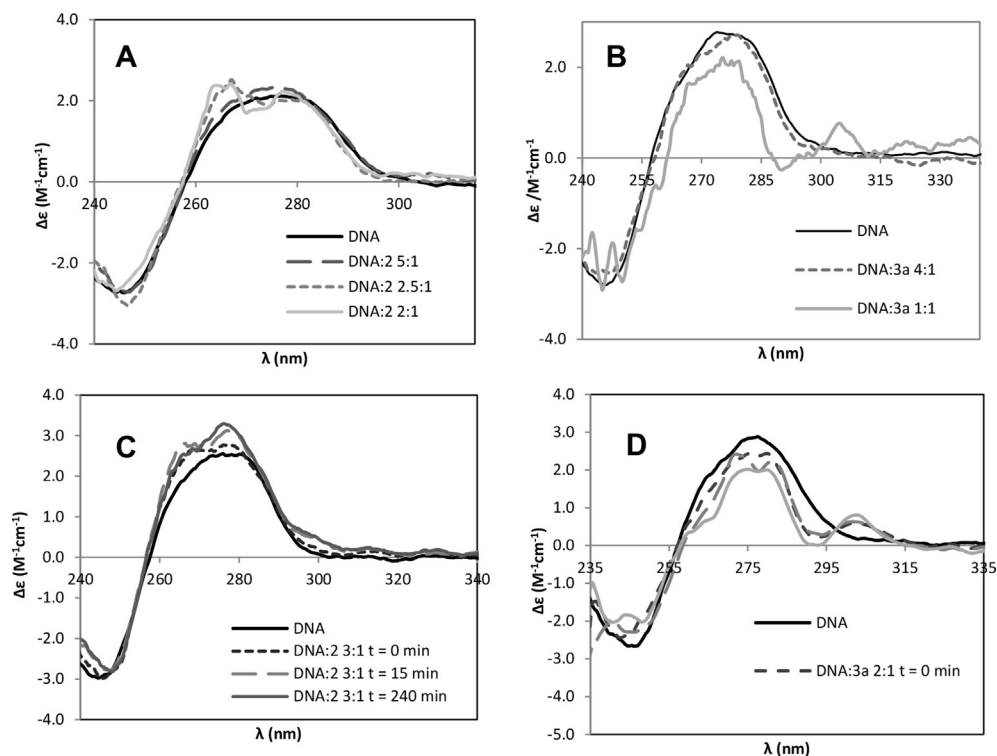


**Fig. 10.** Circular dichroism spectra of ctDNA (ca. 70  $\mu\text{M}$ ) in the absence and in the presence of (A) increasing amounts of **2**,  $[\text{FeL}(\text{phen})]\text{PF}_6$ ; (B) increasing amounts of **3a**,  $[\text{FeL}(\text{amphen})]\text{PF}_6$ ; (C) **2** (23  $\mu\text{M}$ ) with increasing time; (D) **3a** (35  $\mu\text{M}$ ) with increasing time. 10 mm optical path.

### 2.3. DNA binding data

Stock solutions of the complexes were prepared in DMSO. Sample solutions were prepared by dilution of the DMSO stock solution in Hepes buffer. The amount of organic solvent was kept below 4% (v/v). Stock solutions of *Calf Thymus* DNA (ctDNA) were prepared in Hepes buffer (10 mM, pH 7.4). Electronic absorption titrations were done by adding aliquots of the DNA stock solution to solutions of the complexes (30–55  $\mu\text{M}$ ) in 3% DMSO-Hepes. The DNA solution was also added to the reference cell.

Circular dichroism studies were done in quartz SUPRASIL® cuvettes of 10 mm or 5 mm optical path. Hepes buffer or Hepes/DMSO mixtures were used to obtain the baseline, which was subtracted from each spectrum. Spectra were collected from 230 to 500 nm with a resolution of 1 nm band-width, 3 accumulations.

#### 2.3.1. Iodide quenching assay

Stock solutions of  $[\text{Fe}(\text{phen})\text{Cl}_3]$  **7**, in DMSO, were diluted directly in a quartz cuvette of 1 cm path length containing 3 mL of aqueous Hepes buffer (10 mM, pH = 7.4) solution, giving a final concentration of complex of ca. 14.2  $\mu\text{M}$  (0.7% DMSO). Increasing amounts of potassium iodide (final concentrations between 0.4 and 86  $\mu\text{M}$ ) were added directly to the cuvette in the absence and in the presence of ctDNA (100  $\mu\text{M}$ ) and the emission spectra were recorded. All solutions were allowed to equilibrate for 5 min before measurements. Fluorescence emission was recorded between 300 and 500 nm at room temperature with excitation at 295 nm.

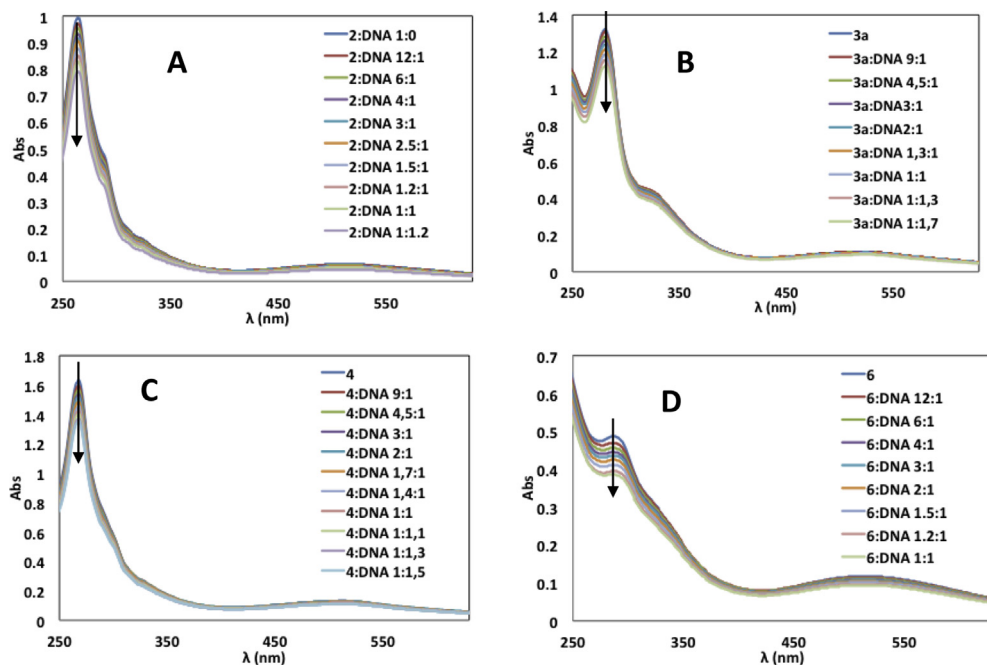


**Fig. 11.** UV-vis absorption spectra of (A) complex 2,  $[\text{FeL}(\text{phen})]\text{PF}_6$ , (31  $\mu\text{M}$ ) and (B) complex 3a,  $[\text{FeL}(\text{amphen})]\text{PF}_6$ , (46  $\mu\text{M}$ ), (C) complex 4,  $[\text{FeL}(\text{Clphen})]\text{PF}_6$ , (46  $\mu\text{M}$ ) and (D) complex 6,  $[\text{FeL}(\text{EtOH})]\text{NO}_3$ , (51  $\mu\text{M}$ ) in 3% DMSO – HEPES 10 mM solution, in the absence and presence of increasing amounts of ctDNA. Solutions develop visible aggregates at complex:DNA ratio 1:1. 10 mm optical path. Arrows indicate increasing DNA concentration.

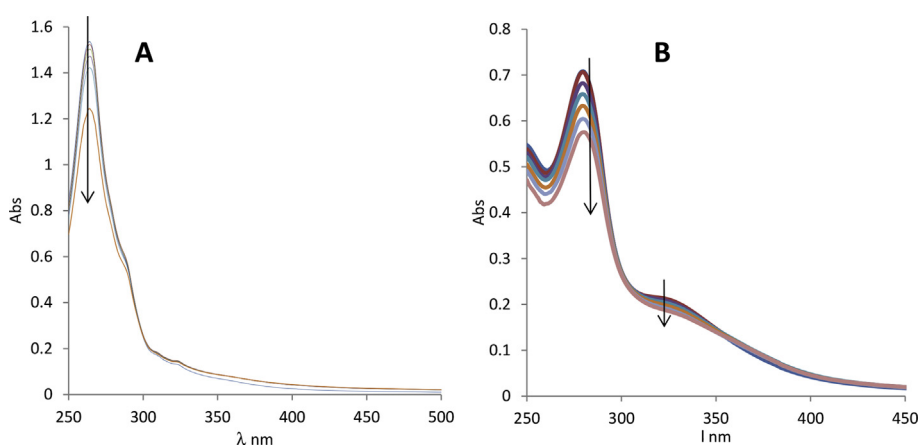


**Fig. 12.** UV-vis absorption spectra of (A) complex 7,  $[\text{Fe}(\text{phen})\text{Cl}_3]$ , (50  $\mu\text{M}$ ) and (B) complex 8,  $[\text{Fe}(\text{amphen})\text{Cl}_3]$ , (25  $\mu\text{M}$ ) in 3% DMSO – HEPES 10 mM solution, in the absence and presence of increasing amounts of ctDNA. 10 mm optical path. Arrows indicate increasing DNA concentration.

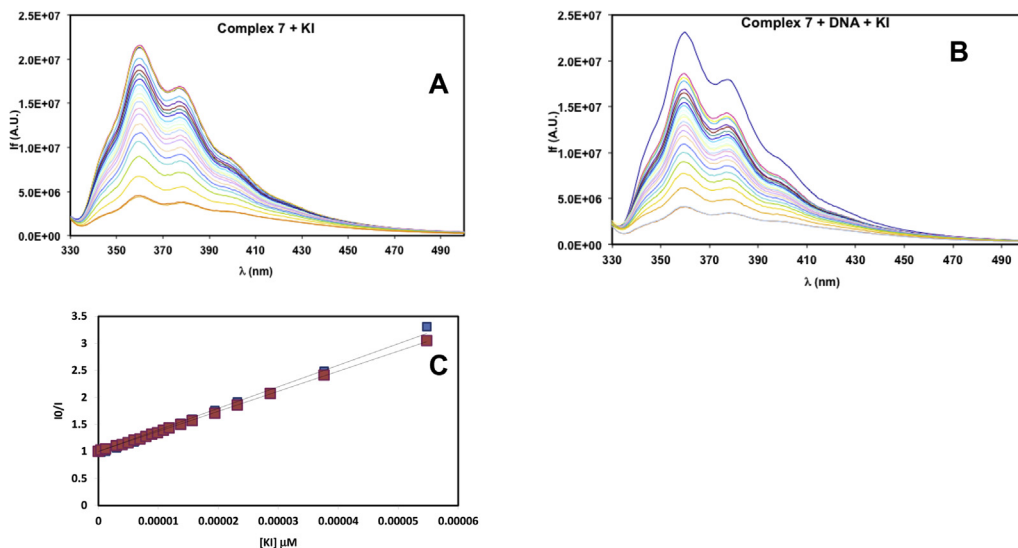


**Fig. 13.** Fluorescence emission spectra ( $\lambda_{exc} = 295$  nm) measured for solutions containing complex **7**,  $\text{Fe}(\text{phen})\text{Cl}_3$ , 14 mM, and increasing amounts of KI (from 0 to 54 mM) in the absence (a) and the presence of *ct*DNA, 100 mM (b). The arrows indicate increasing KI concentrations; in B the blue spectrum is the complex alone and the orange spectrum corresponds to **7** + DNA. c) the Stern-Volmer plot in both experiments: absence (blue,  $R^2 = 0.994$ ) and presence (red,  $R^2 = 0.999$ ) of DNA.

#### 2.4. Cell culturing

HeLa (ATCC, CCL-2), H1299 (ATCC, CRL-5803) and MDA-MB-231 cells (ATCC, HTB-26) grown in Dulbecco's Modified Eagle Medium-F12 (DMEM-F12, Sigma-Aldrich, #D0547) containing 5% FBS (Biochrom, #S0415) and penicillin (100 units/mL) and streptomycin (100  $\mu\text{g}/\text{mL}$ ) (Biochrom, #A2212) in a 37  $^\circ\text{C}$ , 5%  $\text{CO}_2$  incubator.

#### 2.5. Microscopic imaging for morphological changes

$8 \times 10^3$  HeLa, H1299 and MDA-MB-231 cells were seeded on 96 well plates. The day after seeding, cells were treated in serial dilutions of complexes **2**, **3** and **4** (all freshly prepared in cell culture medium), added on the cells, and incubated for 24, 48 or 72 h. The experiment was repeated at two independent times with all cell lines. Images were taken using Differential interference contrast (DIC) microscopy, with a Leica DMI 6000 fluorescence microscope.

#### 2.6. TUNEL assay

$5 \times 10^4$  cells (HeLa and MDA-MB-231) were seeded on 12 mm round cover slips, treated with freshly prepared complexes (**2**, **3** and **4**) at 25  $\mu\text{M}$  for 24 h, and fixed in 4% paraformaldehyde (15 min, RT). "In Situ Cell Death Detection Kit" (Roche, #11767291910) was used for detecting DNA breaks following manufacturer's instructions. The experiment was repeated at two independent times with all cell lines. Images were taken with using Leica DMI 6000 fluorescence microscope (40 X).

#### 2.7. Annexin V/7AAD staining and flow cytometry

$2 \times 10^5$  H1299 and MDA-MB-231 cells were seeded on 6 well plates. The day after seeding, cells were treated with 12.5 and 25  $\mu\text{M}$  of complexes (**2**, **3** and **4**) for 48 h. "Annexin V/Dead Cell kit" (MCH100105, Millipore) was used for detecting cells undergoing apoptosis. Cells were harvested by

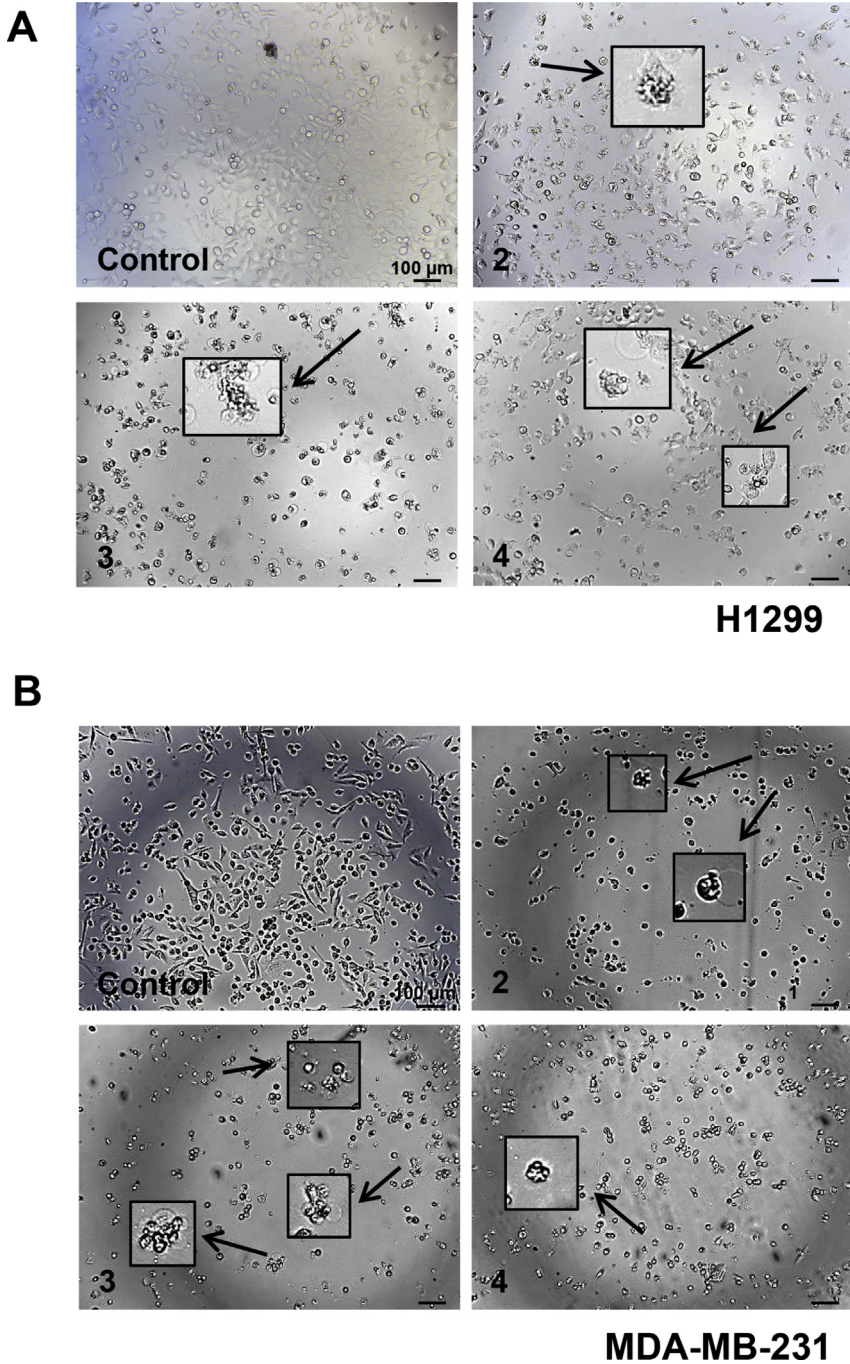


**Fig. 14.** Morphological changes in response to Fe-complexes (2, 3 and 4). H1299 (A) and MDA-MB-231 (B) cells were treated with 12.5  $\mu$ M of Fe-complexes and monitored for changes cell morphology. Insets show enlarged views of representative examples for selected cells exhibiting apoptotic features.

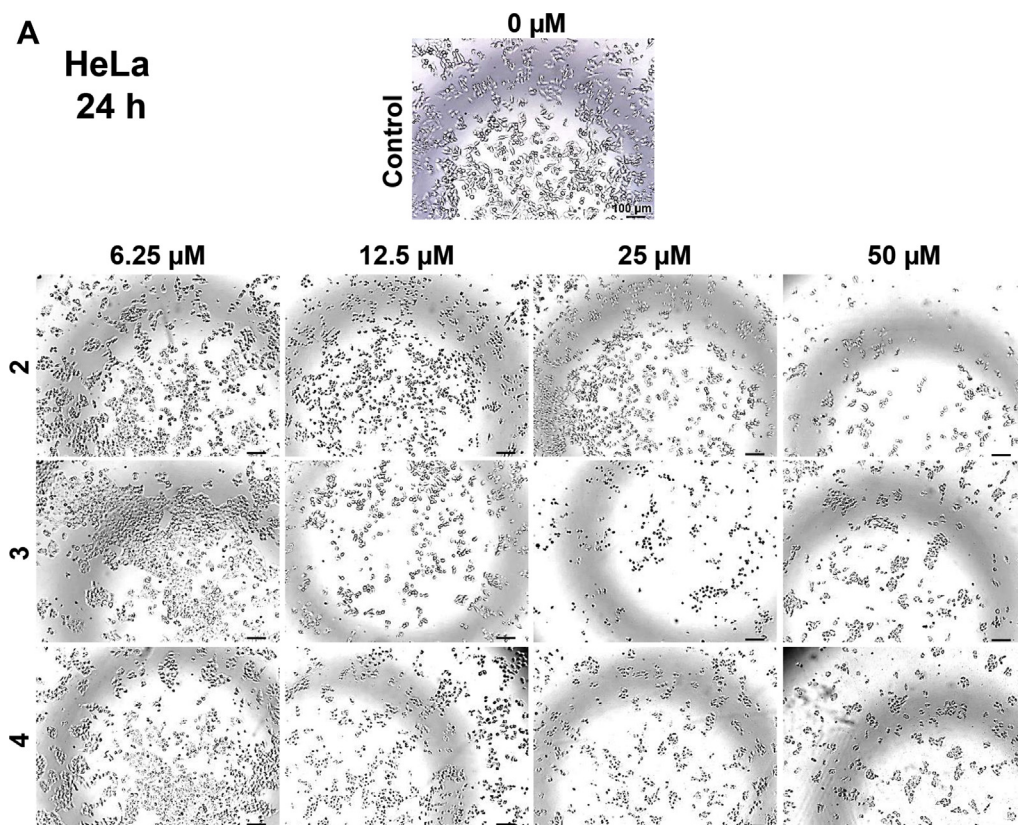


**Fig. 15.** Morphological changes in response to Fe-complexes. HeLa cells were treated with the Fe-complexes (**2**, **3** and **4**) at different concentrations (6.25–50  $\mu\text{M}$ ) for (A) 24 h, (B) 48 h, (C) 72 h.

trypsinisation and resuspended in PBS with 1% FBS at a concentration of  $1 \times 10^5$  cells/mL. The cells were incubated with “Annexin V/Dead Cell Reagent” (RT, 20 min, in dark). The live, dead, early and late apoptotic cells were counted with the Muse Cell Analyzer (Merck Millipore, USA).

### 2.8. Caspase 3/7 activity assay

$1 \times 10^4$  H1299 and MDA-MB-231 cells were seeded on 96 well plates. The day after seeding, cells were treated with 12.5 and 25  $\mu\text{M}$  of freshly prepared complexes (**2**, **3** and **4**) for 24 h. “Caspase-Glo® 3/7 Assay” (Promega, #G8091) was used for measuring caspase-3/7 activity following manufacturer's instructions. In brief, 100  $\mu\text{L}$  of Caspase-Glo® 3/7 Reagent was added to each well, and the plates were incubated on shaker (RT, 300 rpm, 1 h, in dark). Total volume was transferred to white-walled 96-well plates and the luminescent signal was detected using a luminometer (FL $\times$ 800, Bio-Tek, USA). The experiment was repeated using duplicate wells at two independent times with all cell lines, and the results are given in relative fold change to mock treated cells.

### 2.9. $\gamma\text{H2AX}/8\text{-oxo-guanine}$ staining

$5 \times 10^4$  MDA-MB-231 and H1299 cells were seeded on 12 mm round cover slips. The next day, cells were treated with 12.5 and 25  $\mu\text{M}$  of complexes **2**, **3** and **4**, and incubated for 24 h. Cells were then fixed in 4% paraformaldehyde/PBS for 10 min, permeabilized in 0.3% (v/v) Triton-X/PBS for 10 min, and

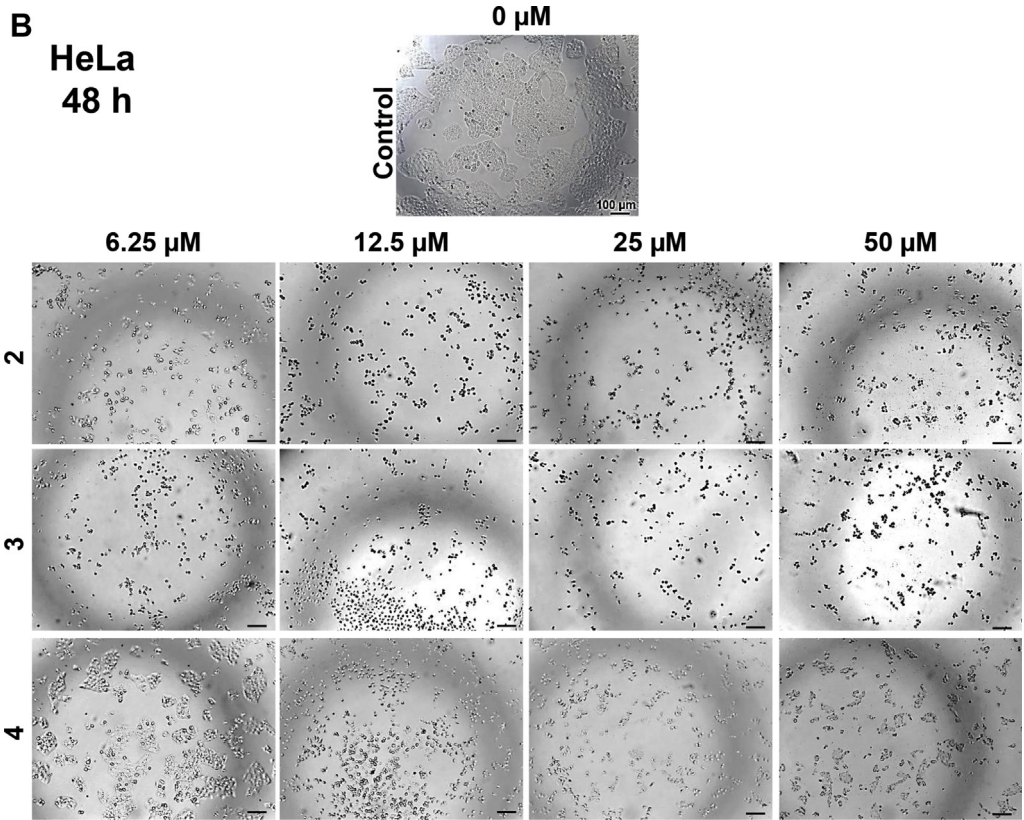


**Fig. 15.** (continued).

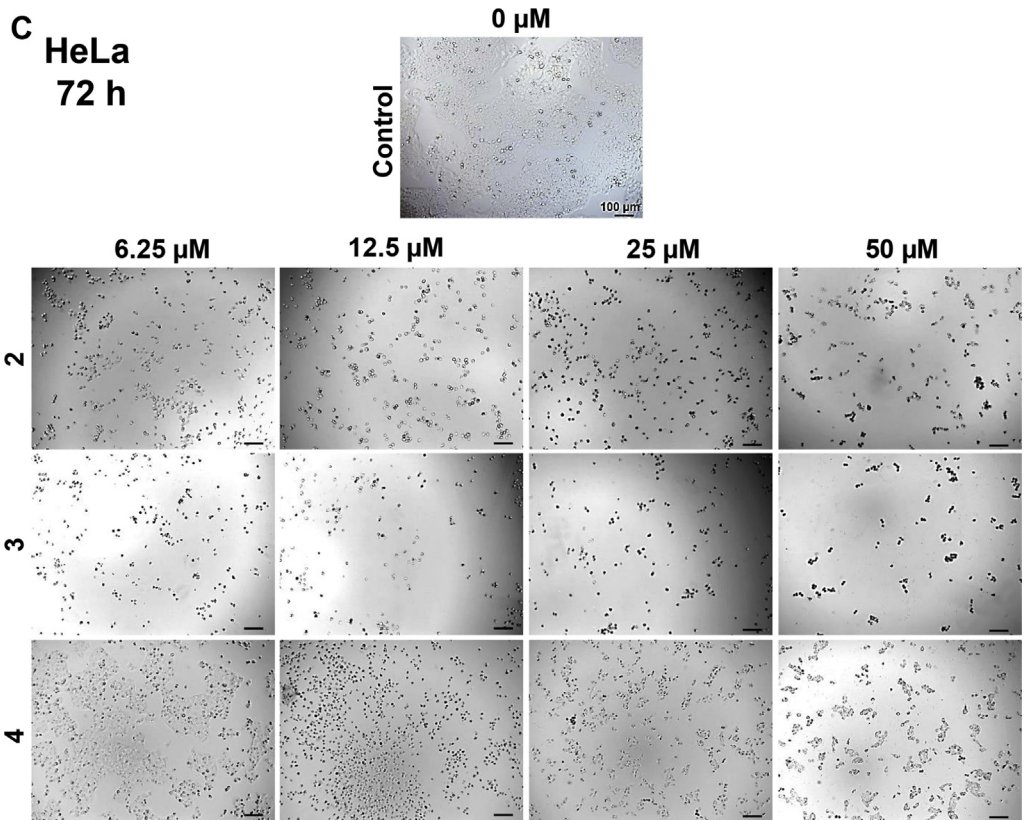


**Fig. 15.** (continued).

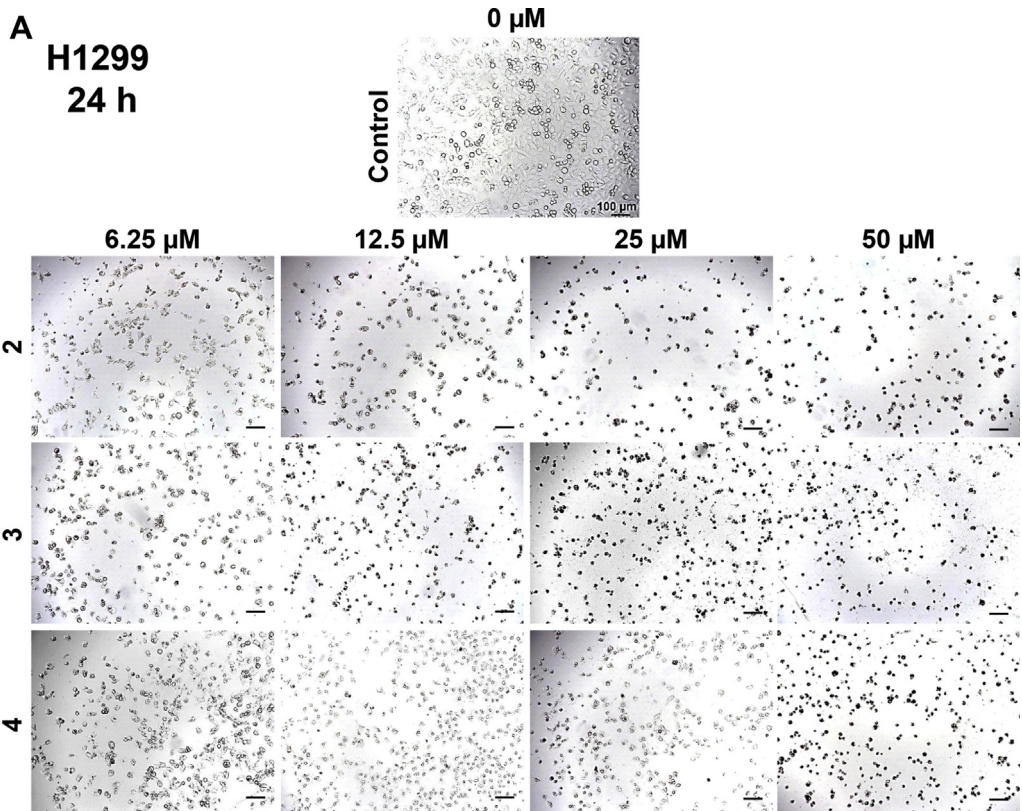


**Fig. 16.** Morphological changes in response to Fe-complexes. H1299 cells were treated with the Fe-complexes (**2**, **3** and **4**) at different concentrations (6.25–50  $\mu\text{M}$ ) for (A) 24 h, (B) 48 h, (C) 72 h.

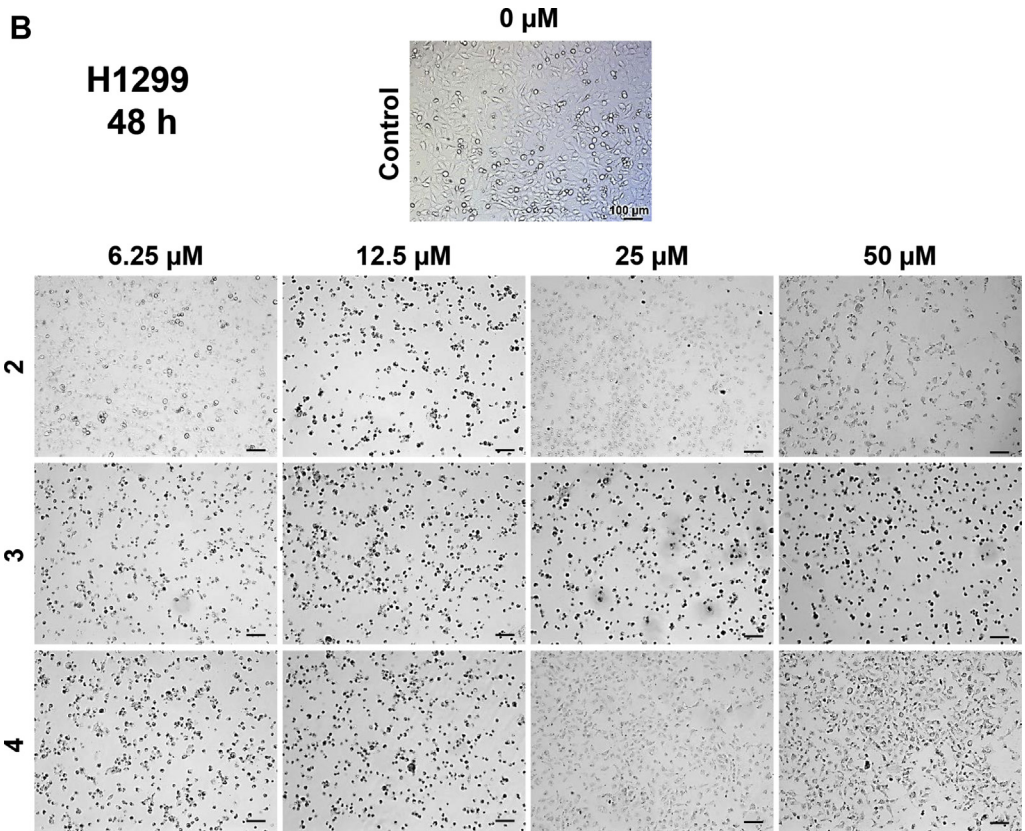


**Fig. 16.** (continued).

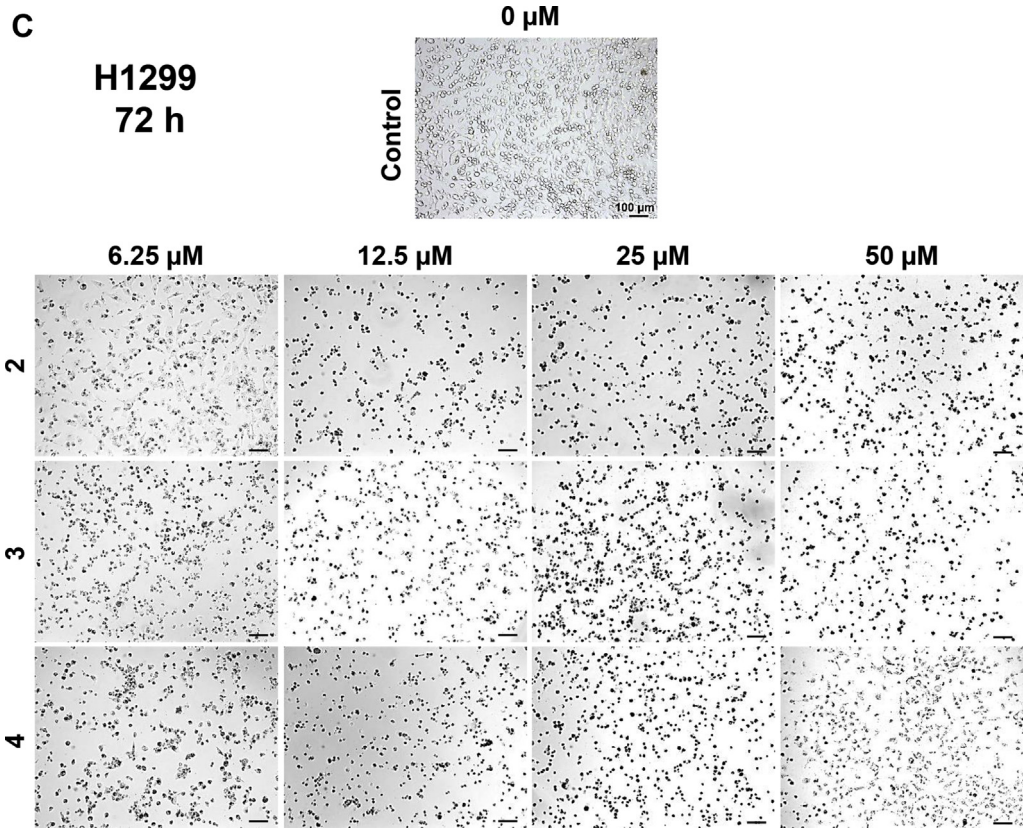


**Fig. 16.** (continued).

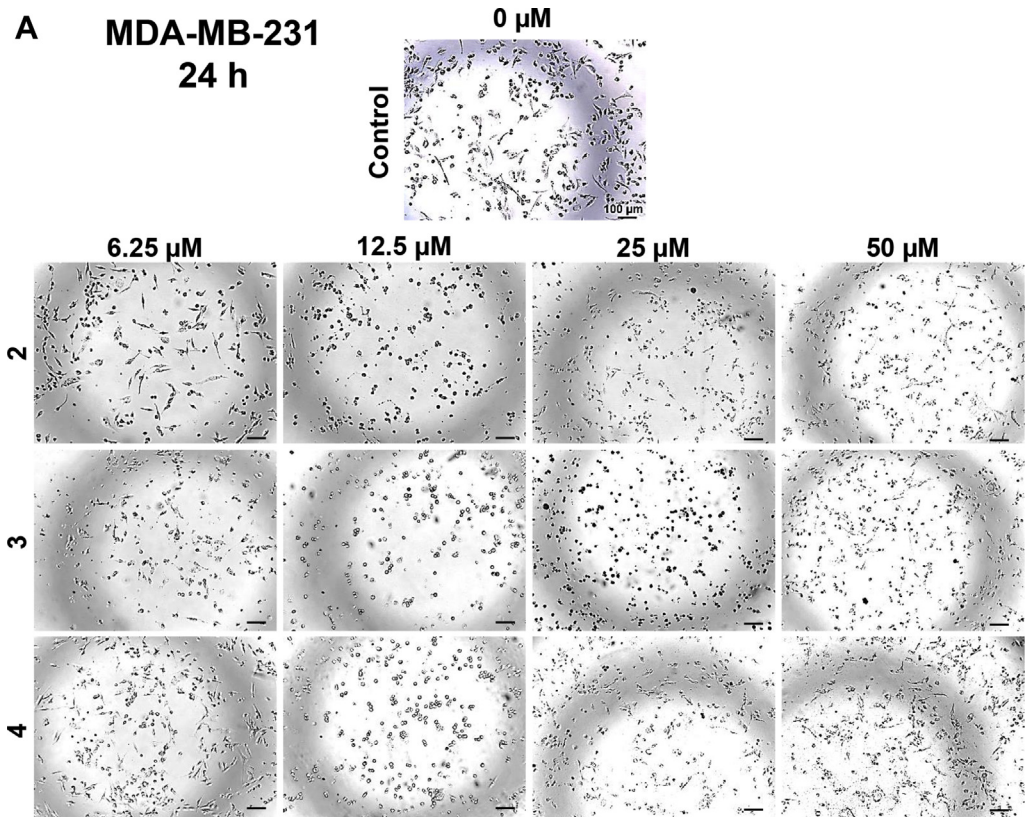


**Fig. 17.** Morphological changes in response to Fe-complexes. MDA-MB-231 cells were treated with the Fe-complexes (**2**, **3** and **4**) at different concentrations (6.25–50  $\mu\text{M}$ ) for (A) 24 h, (B) 48 h, (C) 72 h.

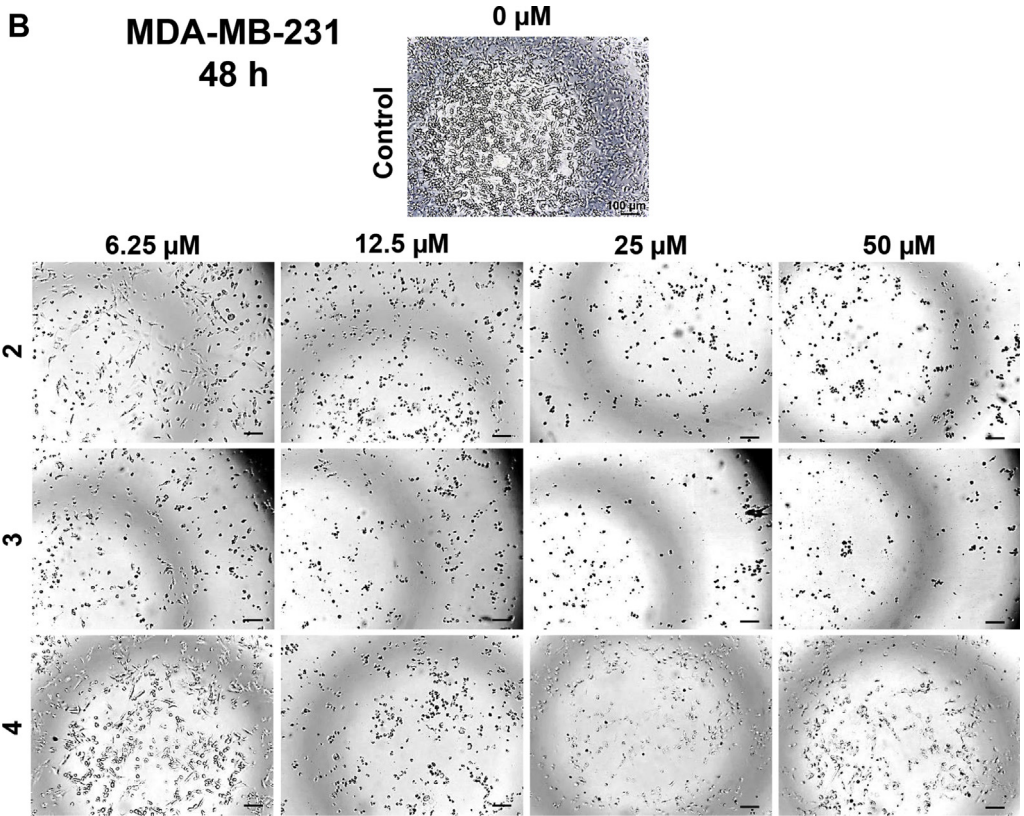


**Fig. 17.** (continued).

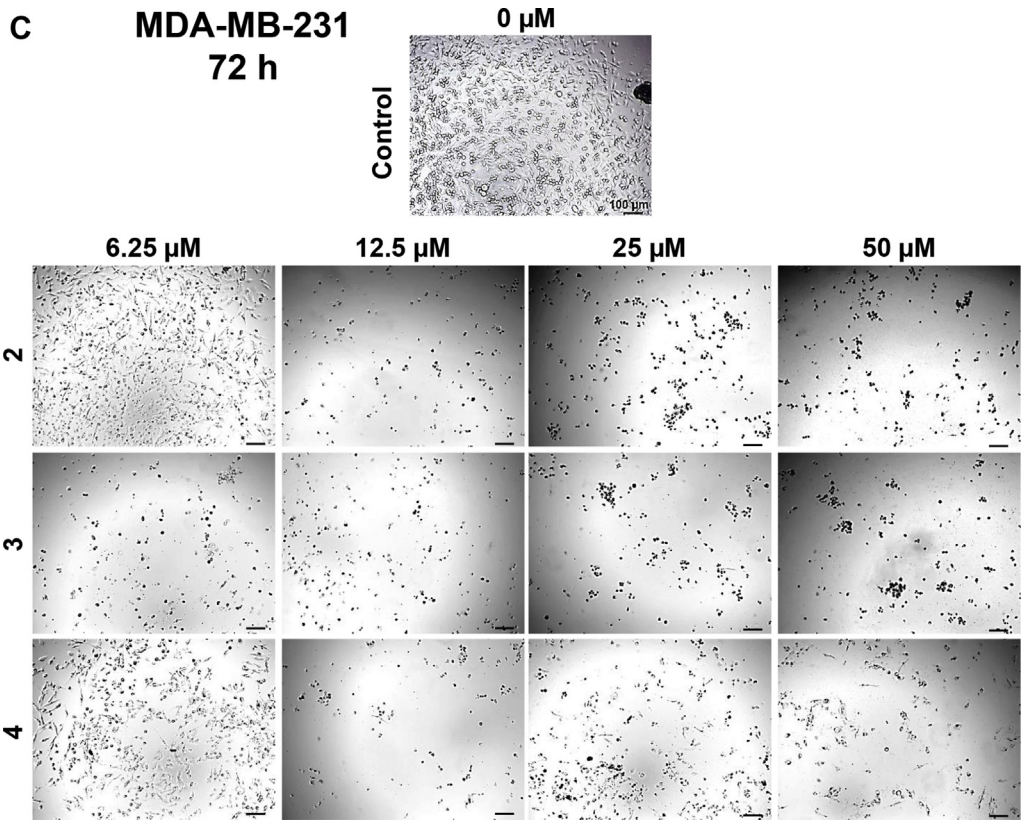
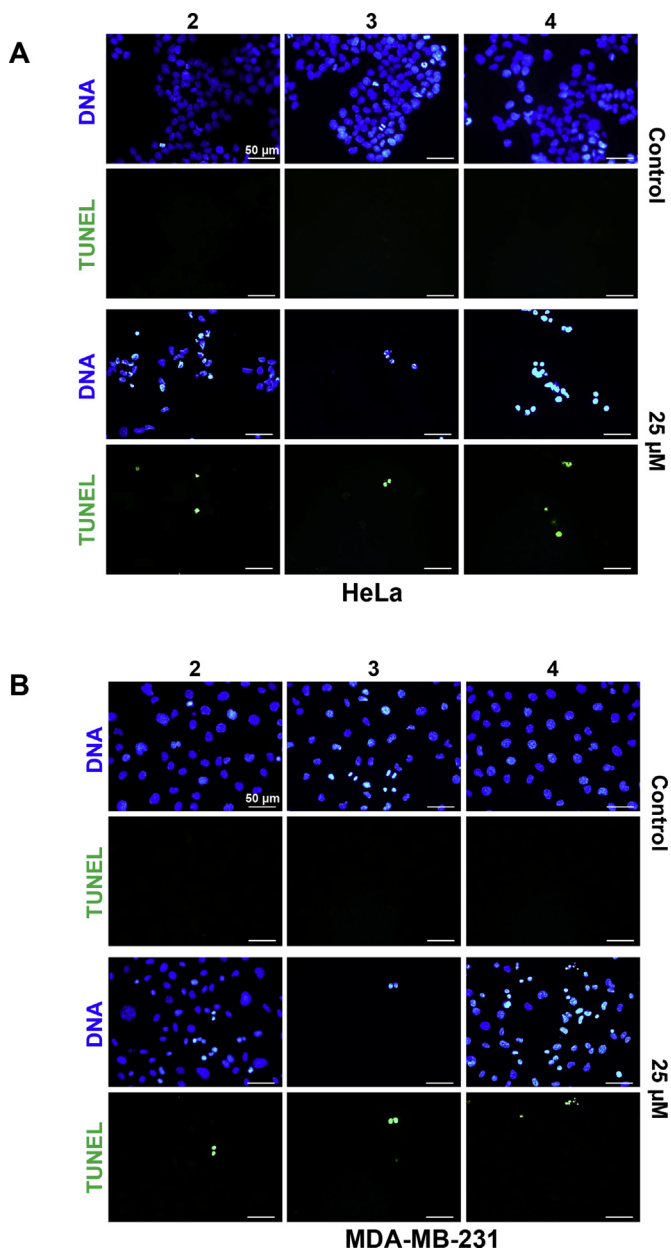
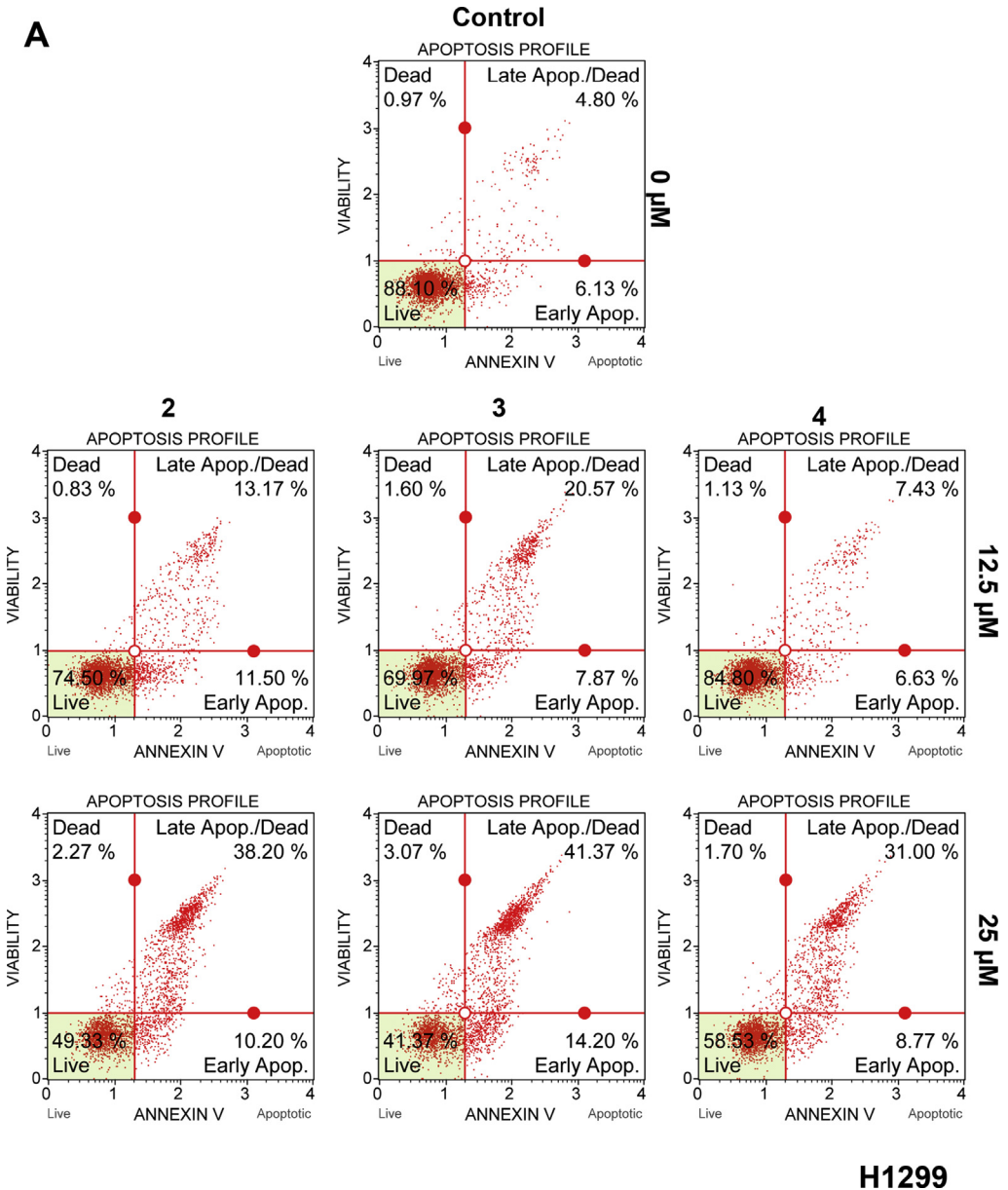


Fig. 17. (continued).



**Fig. 18.** Determination of DNA fragmentation using Terminal deoxynucleotidyl transferase dUTP nick end labeling assay (TUNEL). HeLa (A) and MDA-MB-231 (B) cells were treated with 25 μM of compounds **2**, **3** or **4** (24 h) as indicated at the top of the figures. While mock treated controls exhibited very few to no TUNEL positive nuclei, drug treated cells were labelled green.



**Fig. 19.** Induction of apoptosis as determined by Annexin V staining. H1299 (A) and MDA-MB-231 (B) cells were treated with the Fe-complexes (2, 3 and 4) at a final concentration of 12.5 or 25 μM and assessed for Annexin V positivity as described in materials and methods. Representative flow cytometry plots are shown. 10.000 cells were scored in each analysis. % cells in each quadrant are indicated on the plots.

**B**

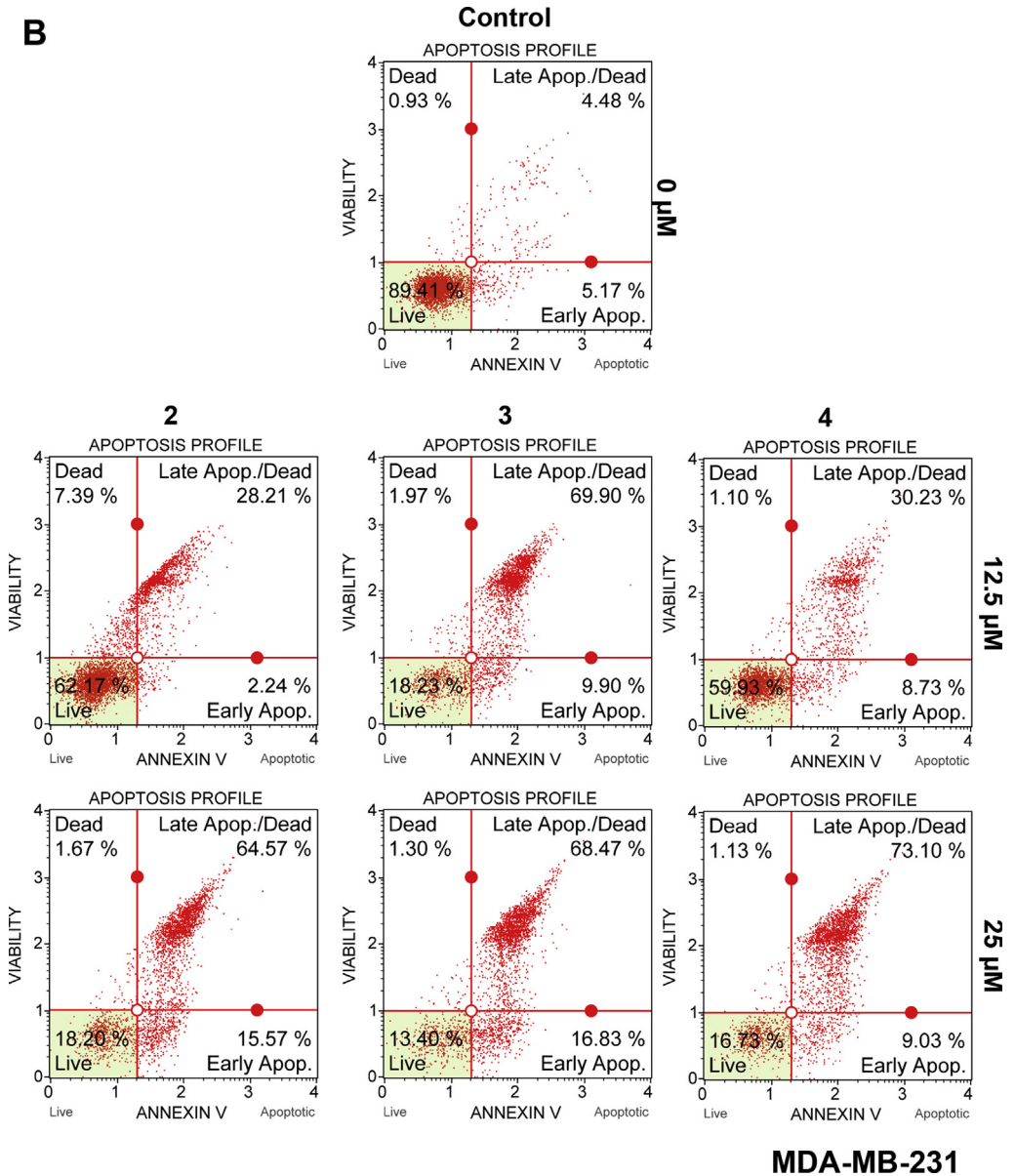


**Fig. 19.** (continued).

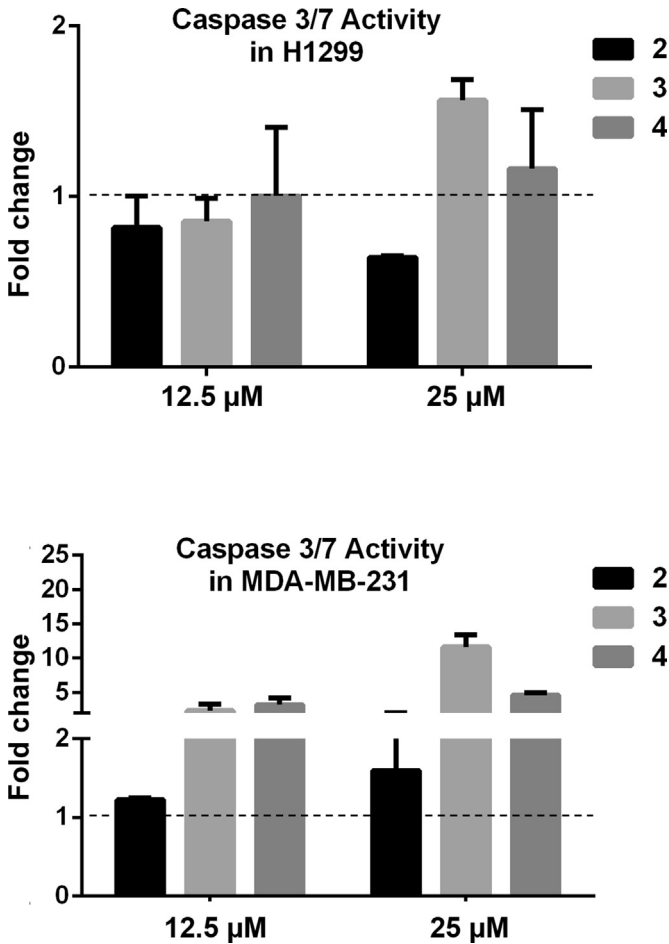


**Fig. 20.** Increase in caspase 3/7 activity in response to Fe-complexes. H1299 and MDA-MB-231 cells were treated with the Fe-complexes (2, 3 and 4) at a final concentration of 12.5 or 25 μM and assessed for caspase 3/7 activity as described in materials and methods. The dashed line indicates 1 fold, the activity measured in the mock treated control cells. The image was drawn using the GraphPad Prism software. x-axis: Drug concentration, y-axis: Fold change relative to mock treated cells.

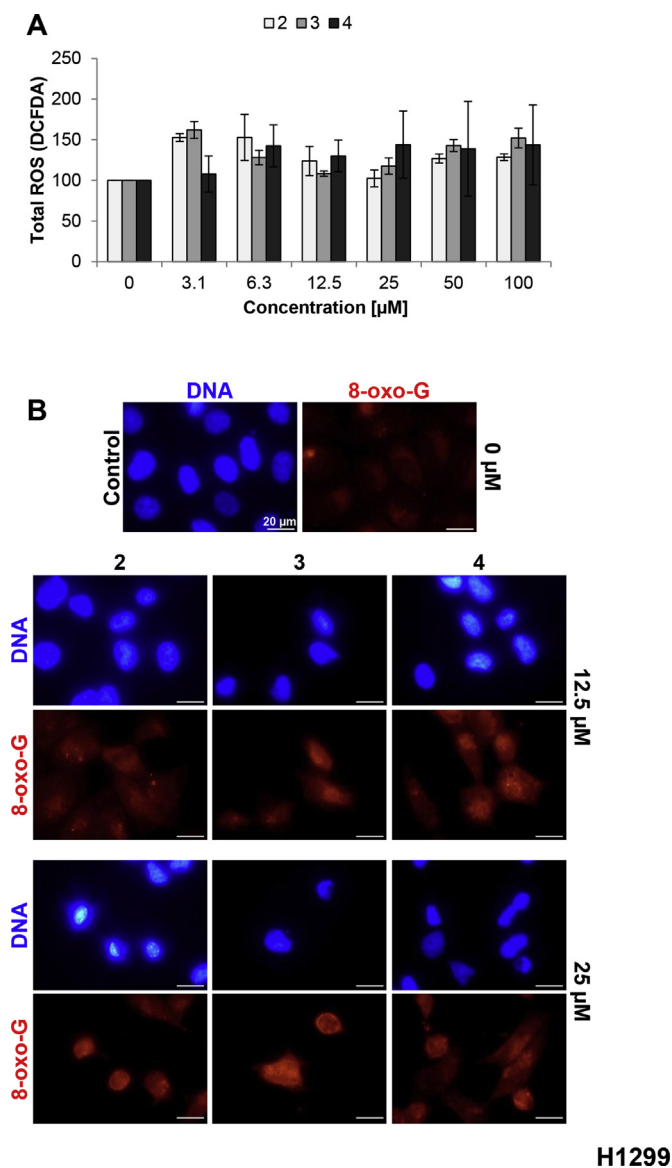


**Fig. 21.** Induction of reactive oxygen species and oxidative DNA damage in response to drug treatment in H1299 cells. (A) Total ROS was increased in a concentration dependent manner with all three drugs. (B) 8-oxo-G staining was used to evaluate oxidative DNA damage. Top panel shows DNA and 8-oxo-G staining of mock treated control cells. A clear increase in 8-oxo-G was visualized following drug treatment at both 12.5 and 25  $\mu$ M.

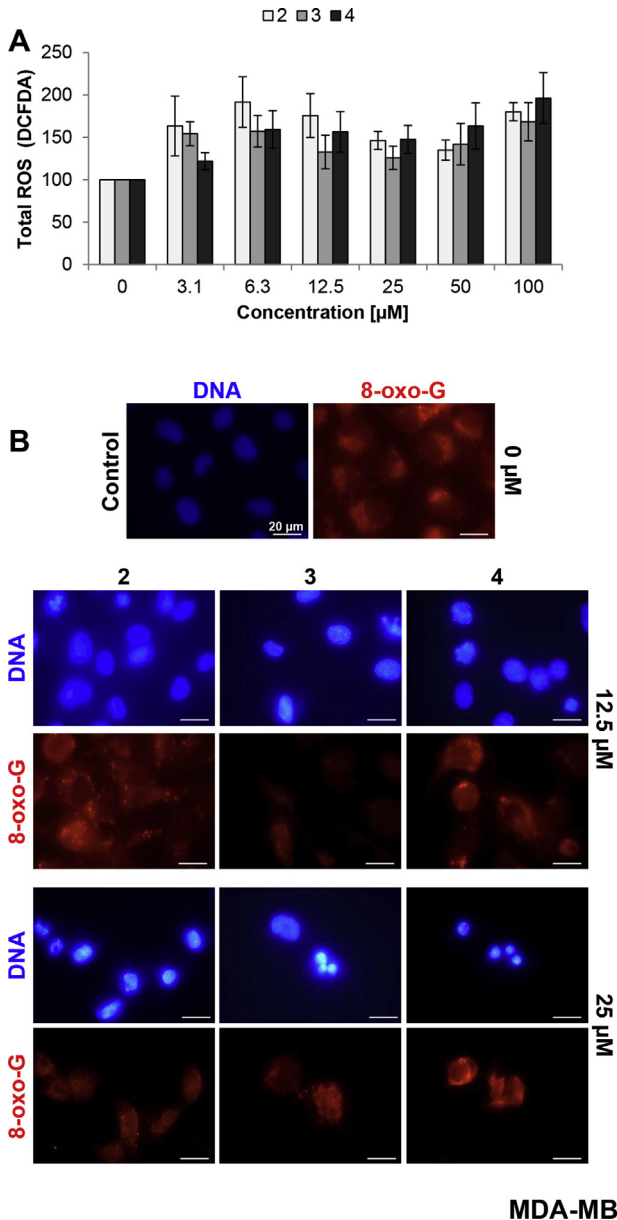


**Fig. 22.** Induction of reactive oxygen species and oxidative DNA damage in response to drug treatment in MDA-MB-231 cells. (A) Total ROS was increased in a concentration dependent manner with all three drugs. (B) 8-oxo-G staining was used to evaluate oxidative DNA damage. Top panel shows DNA and 8-oxo-G staining of mock treated control cells. A clear increase in 8-oxo-G was visualized following drug treatment at both 12.5 and 25 µM.

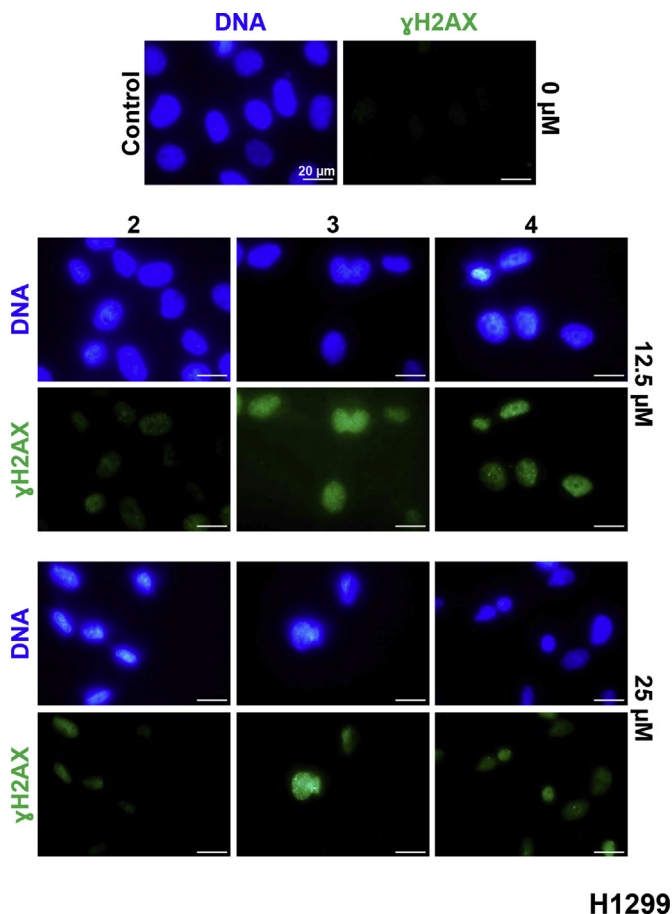


**Fig. 23.** Induction of DSBs as determined by  $\gamma$ H2AX staining. H1299 cells were treated with the Fe-complexes (**2**, **3** and **4**) at a final concentration of 12.5 or 25  $\mu$ M and stained for  $\gamma$ H2AX as described in materials and methods. Representative images are shown.  $\gamma$ H2AX positive cells become evident following drug treatment. DNA is labelled with blue, and  $\gamma$ H2AX is labelled with green fluorescence.

blocked with 1% gelatin in PBS for 1 h. Cells were stained with  $\gamma$ H2AX antibodies (1:400 diluted in 5% BSA/PBS, Cell Signaling mAb #9718) or 8-oxo-G antibodies (1:100, EMD Millipore, MAB3560) at +4 °C, overnight, and with appropriate secondary antibodies (1:500 diluted in 5% BSA/PBS) for 1 h, at RT. The experiment was repeated at two independent times with all cell lines. Images were taken with at 100 X magnification using Leica DMI 6000 fluorescence microscope.

### 2.10. DCFDA (2',7'-dichlorofluorescein diacetate) analysis

$8 \times 10^3$  H1299 and MDA-MB-231 cells were seeded on 96 well plates. The day after seeding, cells were treated in serial dilutions of freshly prepared complexes (**2**, **3** and **4**) and incubated for 24 h. The following day, DCFDA solution (Sigma-Aldrich, #D6883, in PBS) was added on the cells at a final concentration of 5  $\mu$ M and incubated for 20 min at 37 °C in 5% CO<sub>2</sub> incubator. Plates were read at 485 nm (excitation), 535 nm (emission) wavelength using a microplate reader (Biotek Instruments Inc.). The experiment was repeated at two independent times with all cell lines. Fluorescein intensity was normalized to the number of the cells.

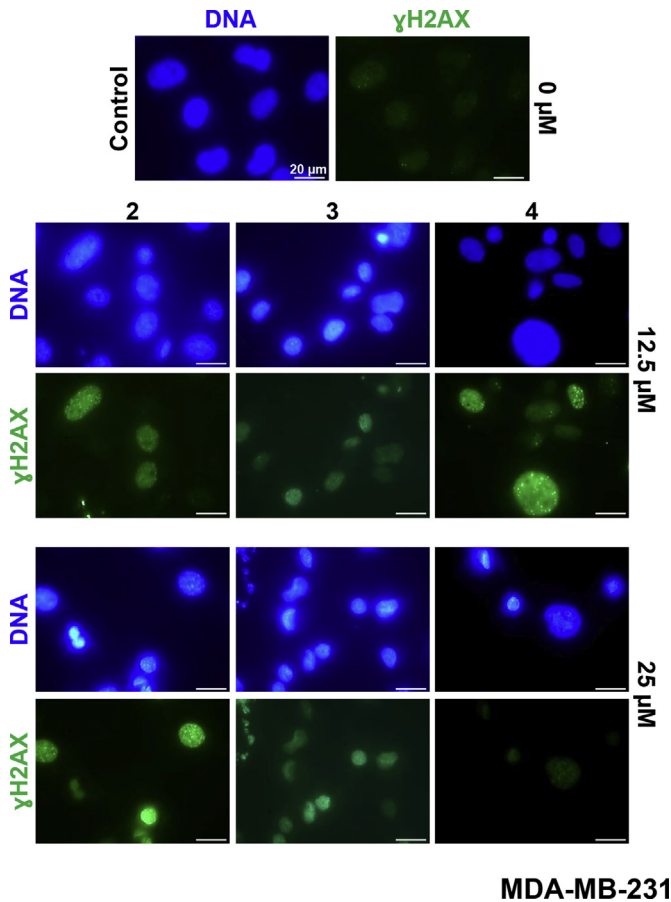


**Fig. 24.** Induction of DSBs as determined by  $\gamma$ H2AX staining. MDA-MB-231 cells were treated with the Fe-complexes **2**, **3** and **4** at a final concentration of 12.5 or 25  $\mu$ M and stained for  $\gamma$ H2AX as described in materials and methods. Representative images are shown.  $\gamma$ H2AX positive cells become evident following drug treatment. DNA is labelled with blue, and  $\gamma$ H2AX is labelled with green fluorescence.

### 2.11. COMET assay

**Dose-Response Relationship:**  $4 \times 10^4$  cells (MDA-MB-231 and H1299) were seeded on 24 well plates. The following day, complexes **2**, **3** and **4** were prepared fresh in culture medium (12.5 and 25  $\mu$ M), added on the cells, and incubated at 37 °C, in 5% CO<sub>2</sub> for 24 h. 'Ethyl methanesulfonate' (EMS, Merck-Millipore, #8.20774.0005, 40 mM, 1 h) was used as positive control. PBS was used as negative control. At the end of treatment, cells were trypsinized, and suspended at a concentration of  $1.6 \times 10^4$  cells/mL.

**Cell lysis and electrophoresis:** The cell suspensions were mixed with low melting agarose (1:3) and spread over the slide. Following jellification of the agarose, the slides were submerged in a covered dish containing lysis solution overnight (18–20 h, 4 °C, dark). The day after, the slides were washed three times (20 min, in alkaline carrier buffer (pH  $\geq$  13)), submerged in fresh alkaline solution, electrophoresed (25 min, 13 V, 0.03 mA), washed with distilled water, and stained with propidium iodide (10  $\mu$ g/mL, 20 min). The slides were analyzed at 535 nm/617 nm wavelength, and the images were taken under fluorescence microscope using 40 X magnification (Leica DMI 6000).

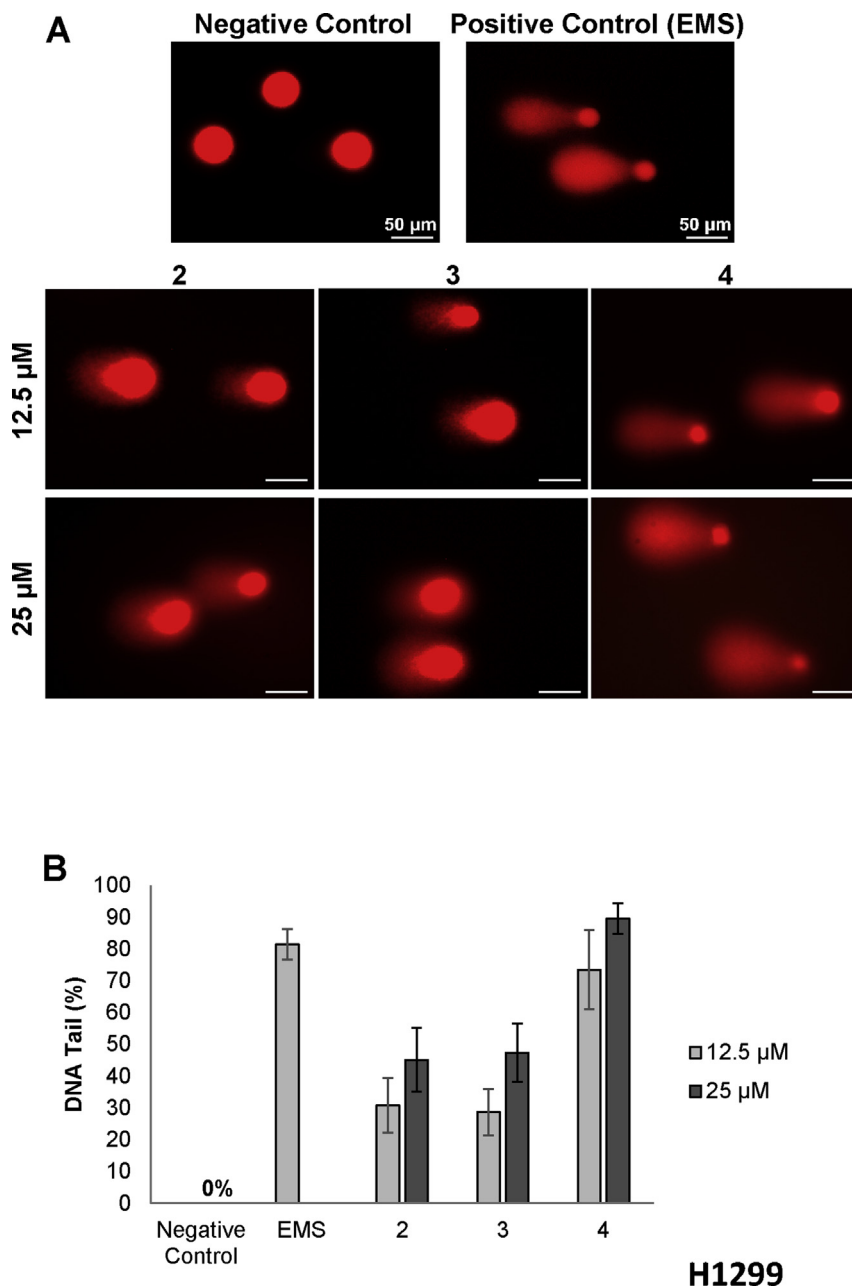


**Fig. 25.** Single-cell gel electrophoresis of H1299 cells following treatment with complexes 2, 3 or 4 at a concentration of 12.5 and 25  $\mu\text{M}$ . Negative control: PBS treated cells, Positive control: Ethyl methanesulfonate (EMS) treated cells (A) Representative microscopic images of cells used for COMET assay (B) Quantification of tail length % based on data from 50 individual cells as described in materials and methods.

Quantitative and qualitative evaluation method: For 'DNA Tail %' calculation, 'head part density' and 'tailing part density' areas were marked using NIH Image J software. The results obtained were

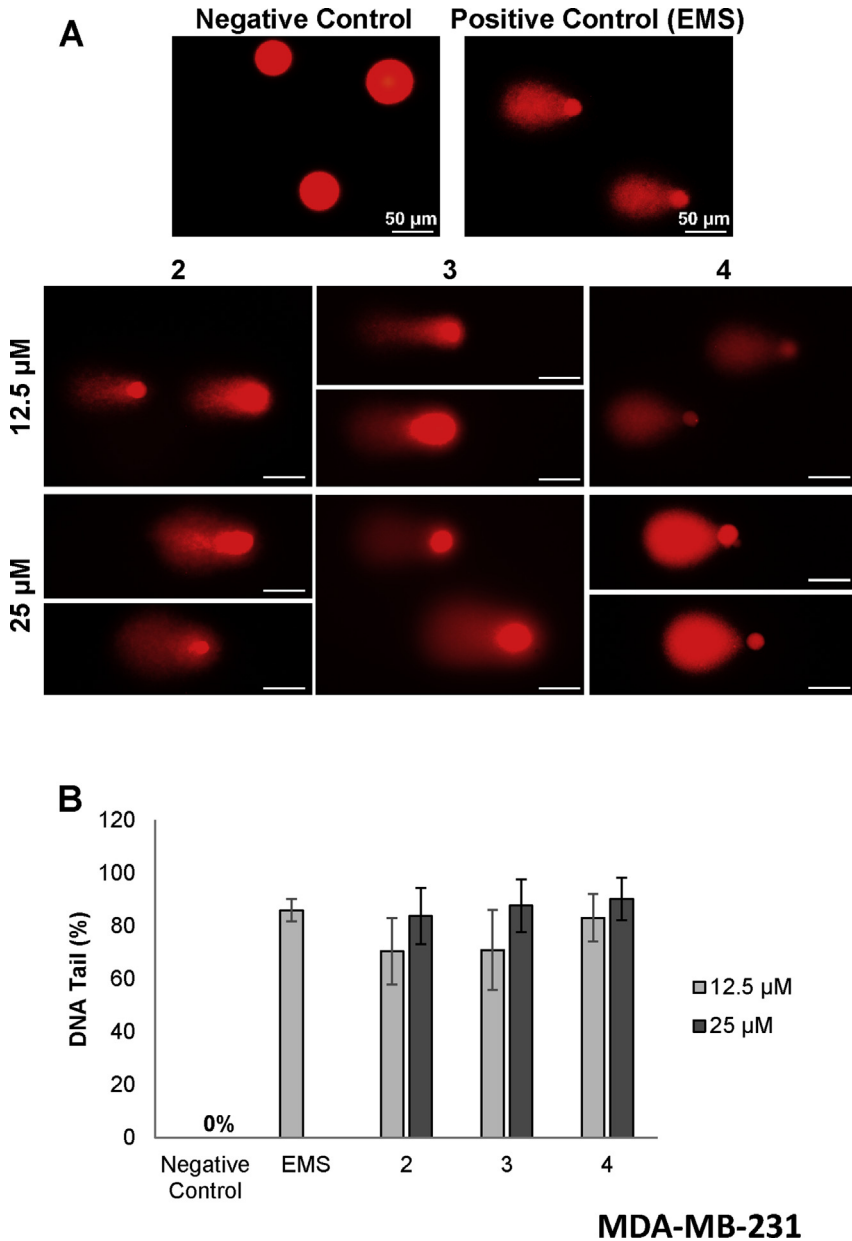


**Fig. 26.** Single-cell gel electrophoresis of MDA-MB-231 cells following treatment with complexes **2**, **3** or **4** at a concentration of 12.5 and 25  $\mu\text{M}$ . Negative control: PBS treated cells, Positive control: Ethyl methanesulfonate (EMS) treated cells (A) Representative microscopic images of cells used for COMET assay (B) Quantification of tail length % based on data from 50 individual cells as described in materials and methods.

calculated by using the following equation; and 50 individual cells were investigated. Two independent biological repeats were performed with similar results.  $\text{DNA Tail \%} = 100 \times \text{Tailing DNA density} / \text{Cell DNA density}$ .

## Acknowledgements

This work was supported by Fundação para a Ciência e a Tecnologia (FCT) (projects UID/QUI/00100/2013, UID/MULTI/04349/2013, UID/BIO/04565/2013, RECI/QEQ-QIN/0189/2012, RECI/QEQ-MED/0330/2012, IF/01179/2013), Programa Operacional Regional de Lisboa (LISBOA-01-0145-FEDER-007317) and programme Investigador FCT (FSE, POPH). The Portuguese NMR and Mass Spectrometry IST–UL Centers are acknowledged for the access to the equipment. The authors thank Fernanda Marques for a preliminary cytotoxicity assessment of the compounds and also Ali Cenk Aksu for calculating the IC<sub>50</sub> values.

This work was supported by Koç University School of Medicine (KUSOM) and the authors gratefully acknowledge use of the services and facilities of the Koç University Research Center for Translational Medicine (KUTTAM), funded by the Republic of Turkey Ministry of Development. The content is solely the responsibility of the authors and does not necessarily represent the official views of the Ministry of Development.

## Conflict of Interest

The authors declare that they have no known competing financial interests or personal relationships that could have appeared to influence the work reported in this paper.

## References

- [1] C.P. Matos, Z. Adiguzel, Y. Yildizhan, B. Cevatemre, T. Bagci Onder, O. Cevik, P. Nunes, L.P. Ferreira, M.D. Carvalho, D.L. Campos, F.R. Pavan, J. Costa Pessoa, M. Helena Garcia, A.I. Tomaz, I. Correia, C. Acilan, May iron(III) complexes containing phenanthroline derivatives as ligands be prospective anticancer agents? *Eur. J. Med. Chem.* 176 (2019) 492–512.
- [2] E. Ulukaya, C. Acilan, Y. Yilmaz, Apoptosis: why and how does it occur in biology? *Cell Biochem. Funct.* 29 (2011) 468–480.